

1 **Development and Performance Assessment of a Novel Plasma p-Tau181 Assay**  
2 **Reflecting Tau Tangle Pathology in Alzheimer's Disease**

3

4 **AUTHORS/AFFILIATIONS:**

5 Kenji Tagai<sup>1,2,7</sup>, Harutsugu Tatebe<sup>1,7</sup>, Sayo Matsuura<sup>1</sup>, Zhang Hong<sup>1</sup>, Naomi Kokubo<sup>1</sup>,  
6 Kiwamu Matsuoka<sup>1</sup>, Hironobu Endo<sup>1</sup>, Asaka Oyama<sup>1</sup>, Kosei Hirata<sup>1</sup>, Hitoshi Shinotoh<sup>1</sup>,  
7 Yuko Kataoka<sup>1</sup>, Hideki Matsumoto<sup>1,3</sup>, Masaki Oya<sup>1</sup>, Shin Kurose<sup>1,4</sup>, Keisuke Takahata<sup>1,4</sup>,  
8 Masanori Ichihashi<sup>1</sup>, Manabu Kubota<sup>1</sup>, Chie Seki<sup>1</sup>, Hitoshi Shimada<sup>1,5</sup>, Yuhei Takado<sup>1</sup>,  
9 Kazunori Kawamura<sup>1</sup>, Ming-Rong Zhang<sup>1</sup>, Yoshiyuki Soeda<sup>6</sup>, Akihiko Takashima<sup>5</sup>,  
10 Makoto Higuchi<sup>1</sup>, Takahiko Tokuda<sup>1\*</sup>

11

12 <sup>1</sup> Institute for Quantum Medical Science, Quantum Life and Medical Science  
13 Directorate, National Institutes for Quantum Science and Technology, Chiba 263-8555,  
14 Japan

15 <sup>2</sup> Department of Psychiatry, The Jikei University of Medicine, Tokyo 105-8461, Japan

16 <sup>3</sup> Department of Oral and Maxillofacial Radiology, Tokyo Dental College, Tokyo  
17 101-0061, Japan

18 <sup>4</sup> Department of Psychiatry, Keio University School of Medicine, Tokyo 160-0016,  
19 Japan

20 <sup>5</sup> Department of Functional Neurology & Neurosurgery, Center for Integrated Human  
21 Brain Science, Brain Research Institute, Niigata University, Niigata 951-8585, Japan

22 <sup>6</sup> Laboratory for Alzheimer's Disease, Department of Life Science, Faculty of Science,  
23 Gakushuin University, Tokyo 171-8588, Japan

24 <sup>7</sup> These authors contributed equally

25 \* Correspondence: [tokuda.takahiko@qst.go.jp](mailto:tokuda.takahiko@qst.go.jp)

26

27

1    **Abstract:** Several blood-based assays for phosphorylated tau (p-tau) have been  
2    developed to detect brain tau pathologies in Alzheimer's disease (AD). However, plasma  
3    p-tau measured by currently available assays is influenced by brain amyloid and,  
4    therefore, could not accurately reflect brain tau deposits. Here, we devised a novel  
5    immunoassay that can quantify N- and C-terminally truncated p-tau fragments  
6    (mid-p-tau181) in human plasma. We measured plasma p-tau181 levels in 164  
7    participants who underwent both amyloid and tau positron emission tomography (PET)  
8    scans using mid-p-tau181 and conventional p-tau181 assays. The mid-p-tau181 assay  
9    displayed stronger correlations with tau PET accumulation than the conventional assay  
10   in the AD continuum and accurately distinguished between tau PET-positive and  
11   -negative cases. Furthermore, the mid-p-tau181 assay demonstrated a trajectory similar  
12   to tau PET alongside cognitive decline. Consequently, our mid-p-tau181 assay could be  
13   useful in evaluating the extent of brain tau burden in AD.

14

15    **Keywords:** Plasma biomarker, Tau phosphorylated at threonine 181 (p-tau181), Simoa,  
16    Tau PET, Alzheimer's disease

17

18

19

20

21

22

23

24

25

26

27

28

29

30

31

32

33

34

35

36

## 1 **Introduction**

2 Estimates project that the number of people with dementia worldwide will reach  
3 153 million by 2050<sup>1</sup>, highlighting the urgent need to address the remarkable health and  
4 social impacts of this condition. Alzheimer's disease (AD), the most prevalent form of  
5 dementia, has been characterized as the deposit of two abnormal proteins, namely  
6 amyloid- $\beta$  (A $\beta$ ) and tau, in the brain. Over the years, numerous disease-modifying  
7 therapies (DMTs) targeting these abnormal proteins have been developed<sup>2</sup>, with the  
8 Food and Drug Administration (FDA) having recently approved several DMTs targeting  
9 A $\beta$  due to their efficacy in decreasing brain amyloid deposition and modestly slowing  
10 AD progression<sup>3-5</sup>. Researchers anticipate that these DMTs will be increasingly utilized  
11 in clinical practice, with the potential for developing additional DMTs targeting not only  
12 A $\beta$  but also tau in the near future<sup>6</sup>.

13 Biomarkers have become an integral part of clinical trials on DMTs given their  
14 widespread use for subject recruitment and outcome measurements<sup>2</sup>. The  
15 amyloid/tau/neurodegeneration (A/T/N) biomarker classification system had been  
16 proposed for the biological staging of AD<sup>7</sup>. In particular, positron emission tomography  
17 (PET) has emerged as a well-established imaging biomarker for assessing the  
18 accumulation of A $\beta$  and tau in the brain<sup>8</sup>, playing a critical role in evaluating novel  
19 DMTs<sup>4,9</sup>. The noteworthy decline in amyloid accumulation based on PET findings<sup>10</sup>  
20 may have expedited the FDA approval of aducanumab<sup>2</sup>. Moreover, incorporating tau  
21 PET as a screening measure, assuming that high tau accumulation may cause resistance  
22 to anti-amyloid therapy, may have played a part in the success of the donanemab  
23 clinical trial<sup>4,11</sup>. Despite their usefulness, PET scans are not ideal for frequent  
24 assessment or large-scale screening given their limited availability, high cost, and  
25 radiation exposure<sup>12</sup>. Similarly, A $\beta$  and p-tau in the cerebrospinal fluid (CSF) have also  
26 been accepted as standard biomarkers for qualifying AD pathology<sup>13,14</sup>. However, CSF  
27 testing has seen somewhat limited use considering its invasiveness, low-throughput  
28 nature, and need for expertise during CSF sampling<sup>12,15</sup>. Based on the present  
29 circumstances surrounding the development of biomarkers for AD, one of the most  
30 critical unmet needs has been the identification of blood-based biomarkers closely  
31 correlated with tau PET parameters that reflect brain tau burden, especially in the  
32 context of selecting suitable patients for anti-amyloid therapies.

33 Recent advances in measurement methodologies have made it possible to quantify  
34 minute amounts of proteins in the peripheral blood that are associated with brain  
35 diseases, thereby enabling the feasibility of blood-based biomarkers<sup>15</sup>. Notably, there is  
36 growing evidence for the clinical significance of plasma phosphorylated tau (p-tau)

1 assays in detecting AD pathology<sup>16–19</sup>, similar to CSF biomarkers. The C-terminal  
2 portion of the tau protein, which predominantly constitutes neurofibrillary tangles<sup>20</sup>, is  
3 seldom detectable in biofluids<sup>21–23</sup>. Most of the current immunoassays for plasma p-tau,  
4 therefore, employ a pair of antibodies, one of which recognizes the phosphorylated  
5 residues, such as Thr181, Thr217, and Thr231, in the mid-portion, while the other  
6 identifies the N-terminal region of the tau protein. Accordingly, currently available  
7 immunoassays for plasma p-tau detect C-terminally truncated p-tau containing the  
8 N-terminus to the mid-domain (N-p-tau)<sup>12</sup>. Plasma p-tau levels quantified using these  
9 N-p-tau assays can accurately differentiate between AD pathology and other tauopathies  
10 with high diagnostic accuracy<sup>17,18,24,25</sup> and help predict future cognitive decline from  
11 prodromal phases<sup>26,27</sup>. However, one of the significant problems in the clinical use of  
12 N-p-tau assays is their inability to be considered as a surrogate marker for tau burden in  
13 the brain<sup>28</sup> given that the measurements obtained had a more pronounced association  
14 with amyloid PET than with tau PET<sup>29–32</sup>. Therefore, the need for developing  
15 blood-based tau biomarkers strongly correlated with PET-detectable tau accumulations  
16 in the brain remains unmet.

17 The present study aimed to formulate a novel p-tau assay that can be  
18 interchangeable with the tau PET study. Considering that the truncation of the  
19 N-terminal of the tau protein may occur subsequent to the truncation of its C-terminal  
20 with the formation of neurofibrillary tangle<sup>33</sup>, we hypothesized that the levels of both N-  
21 and C-terminally truncated p-tau181 fragments could be correlated with the abundance  
22 of tau aggregates in the brain. Thus, we developed a novel mid-region-directed p-tau181  
23 assay by modifying the formerly established N-p-tau181 assay<sup>16</sup>. To validate our  
24 hypothesis, we collected plasma samples from subjects who underwent PET with both  
25 <sup>11</sup>C-Pittsburgh Compound B (<sup>11</sup>C-PiB) and <sup>18</sup>F-florzorotau (aka PM-PBB3/APN-1607)  
26 for the examination of A $\beta$  and tau depositions in the brain, respectively.<sup>34,35</sup> We  
27 demonstrated a strong correlation of between plasma levels of p-tau181 fragments  
28 measured using our mid-region-directed assay (hereinafter called mid-p-tau181) and tau  
29 PET tracer retention but no linear correlation between plasma N-p-tau181 levels and tau  
30 PET data, suggesting the clinical usefulness of the novel assay as a surrogate biomarker  
31 for PET-visible tau pathologies.

32

## 33 **Results**

### 34 ***Validation of the newly developed mid-p-tau181 assay***

35 The plasma mid-p-tau181 assay exhibited high analytical performance (Supplementary  
36 Methods and Results, Supplementary Tables 1–3, Supplementary Figures 1–5), with high

1 precision within and between runs. Spike recovery experiments and parallelism of  
2 serially diluted plasma samples confirmed the reliability of the measurements.

3

#### 4 ***Demographic data***

5 Table 1 summarizes the demographic information of the participants. All participants (n  
6 = 164) underwent neuropsychological assessment, including the Clinical Dementia  
7 Rating (CDR) scale, Mini-Mental State Examination (MMSE), and frontal assessment  
8 battery (FAB), simultaneous amyloid and tau PET imaging, and blood sampling on the  
9 day of the PET examination. Cognitively normal (CN) individuals exhibiting negative  
10 results on amyloid and tau PET imaging were designated into the CN cohort. Patients  
11 with mild cognitive impairment (MCI) and AD who had positive amyloid PET findings  
12 were categorized into the AD continuum group (dubbed AD group). Furthermore,  
13 subjects with progressive supranuclear palsy (PSP) and other frontotemporal lobar  
14 degeneration (FTLD) who had negative amyloid PET findings were classified into the  
15 PSP and FTLD cohorts, respectively. No significant differences in age, years of  
16 schooling, and gender were observed among the groups. All patient groups showed lower  
17 MMSE (CN,  $29.3 \pm 1.0$ ; AD,  $21.9 \pm 4.1$ ; PSP,  $24.8 \pm 5.8$ ; FTLD,  $23.8 \pm 6.1$ ) and FAB  
18 scores (CN,  $16.7 \pm 1.2$ ; AD,  $13.0 \pm 3.0$ ; PSP,  $12.0 \pm 3.6$ ; FTLD,  $11.0 \pm 4.8$ ) than the CN  
19 group ( $p < 0.05$ , Table 1). Notably, 90% of the AD group comprised subjects with  
20 early-stage AD who had a CDR score of 0.5 or 1 accounted; however, the mean MMSE  
21 scores of this group were lower than those of the PSP group ( $p < 0.05$ , Table 1) but did not  
22 significantly differ from those of the FTLD group.

23

#### 24 ***Significant linear correlation between plasma mid-p-tau181 but not N-p-tau181 with 25 tau PET findings in patients with AD continuum***

26 We found a significant linear correlation between the plasma mid-p-tau181 levels and tau  
27 PET tracer retention in patients with AD continuum (Figure 1). Voxel-wise analyses  
28 revealed a positive correlation between plasma mid-p-tau181 levels and tracer binding in  
29 the temporal and parietal cortices [Figure 1A;  $p < 0.05$ , corrected for family-wise error  
30 (FWE)]. This finding was corroborated by the following three different quantitative  
31 indices based on a region of interest (ROI): (1) standardized uptake value ratio (SUVR)<sup>36</sup>  
32 in the temporal meta-ROI that characterizes tau lesions in AD<sup>37</sup>; (2) AD tau score, which  
33 is a machine learning-based measure indicating AD-related features of tau PET images<sup>35</sup>;  
34 and (3) Braak staging SUVRs based on the neuropathological hypothesis<sup>36</sup>  
35 (Supplementary Figure 6). These AD signature ROI analyses revealed significant linear  
36 correlations between plasma mid-p-tau181 levels and temporal meta-ROI SUVRs ( $r =$

1 0.506;  $p = 0.0003$ ), AD tau scores ( $r = 0.556$ ;  $p = 0.0003$ ), and SUVRs in the Braak stage  
2 III/IV limbic ( $r = 0.403$ ;  $p = 0.003$ ) and V/VI neocortical ( $r = 0.508$ ;  $p = 0.0003$ ) but not  
3 Braak stage I/II entorhinal ( $r = 0.216$ ;  $p = 0.149$ ) ROIs. These findings clearly  
4 demonstrate that plasma mid-p-tau181 levels could accurately reflect AD-related tau  
5 accumulation that spreads from the entorhinal cortex first to the inferior temporal lobe  
6 and then to the parieto-occipital regions of the neocortex but not tau accumulation in the  
7 Braak I/II region.

8 Conversely, the conventional N-p-tau181 assay (Simoa pTau-181 Advantage V2.1  
9 kit, Quanterix, MA, USA) showed no significant linear correlations with tau PET tracer  
10 retention (Figure 2). Voxel-based analysis revealed a weak correlation between the  
11 aforementioned parameters in the temporal cortex (Figure 2A;  $p < 0.05$ , uncorrected);  
12 however, no significant correlation was observed upon correction for multiple  
13 comparisons ( $p < 0.05$ , FWE-corrected). Moreover, none of the three ROI-based analyses  
14 revealed significant linear correlations between N-p-tau181 levels and PET parameters ( $p$   
15  $< 0.05$ , after Bonferroni's correction). Instead, these examinations showed inverse  
16 U-shaped nonlinear correlations between plasma N-p-tau181 levels and tau PET SUVRs  
17 in the temporal meta-ROI ( $R^2 = 0.402$ ), AD tau score ( $R^2 = 0.147$ ), and Braak stage III/IV  
18 ( $R^2 = 0.307$ ) and V/VI ROIs ( $R^2 = 0.223$ ) but not Braak stage I/II ROIs (Figure 2B, C).

19

### 20 ***Discriminating between tau PET statuses using plasma mid-p-tau181 levels***

21 Using three different ROI-based methods, we qualitatively assessed the PET-detectable  
22 tau burden in the CN subjects and AD continuum patients. Thereafter, receiver operating  
23 characteristic (ROC) curve analyses were conducted to determine plasma mid-p-tau181  
24 cutoff levels for discriminating between individuals with positive and negative AD-type  
25 tau PET findings. The PET finding classification was based on the cutoff values of  
26 imaging-based Braak staging, temporal meta-ROI SUVR, and AD tau score. The Braak  
27 stage in each subject was determined according to the ROI with the highest Z-score (see  
28 Methods for detailed procedures), with stages 0 and I/II indicating tau-negative and  
29 stages III/IV and V/VI being classified as tau-positive (Supplementary Table 4). The  
30 cutoff values for the meta-ROI SUVR and AD tau score were determined using ROC  
31 curve analyses in the current and previous studies<sup>35</sup>, respectively. Consequently, our  
32 findings showed that tau-positive AD cases had significantly higher plasma  
33 mid-p-tau181 concentrations than did tau-negative AD and CN cases (Figure 3A;  $p <$   
34  $0.0001$ ). Furthermore, area under the ROC curve (AUC) values during ROC analyses of  
35 mid-p-tau181 levels to different between tau PET positivity and negativity defined by  
36 all three methods exceeded 0.85 (Table 2, Figure 3B), indicating that this plasma

1 biomarker with reference to PET-based classifications had robust discriminative power.

2

3 ***Head-to-head comparisons between two p-tau181 assays according to their correlation***  
4 ***with non-tau imaging biomarkers***

5 Next, we examined whether plasma p-tau181 levels determined by either the  
6 pre-established or newly developed assay were correlated with the abundance of  
7 cerebral amyloid accumulations evaluated using PiB-PET (Supplementary Figure 7).  
8 Notably, none of the measures obtained using these p-tau181 assays were correlated  
9 with voxel-based and ROI-based quantitative values of amyloid burden. Meanwhile,  
10 voxel-based morphometry revealed significant negative correlations between the plasma  
11 mid-p-tau181 concentration and gray matter volume in the neocortex, primarily in the  
12 temporal and parietal areas (Figure 4). The ROI-based analysis also confirmed a  
13 correlation between mid-p-tau181 and cortical thinning in AD-signature regions defined  
14 as described elsewhere<sup>38</sup> ( $r = -0.406$ ;  $p = 0.005$ ). In contrast, N-p-tau181 did not exhibit  
15 any correlation with structural imaging measures.

16

17 ***Comparison among blood-based biomarkers according to diagnostic performance for***  
18 ***AD***

19 Figure 5A illustrates group comparisons of four AD-related plasma biomarkers,  
20 including the mid-p-tau181 measured using our in-house assay, ~~with~~ and the  
21 corresponding values for each diagnostic group being presented in Table 1. Our results  
22 indicated significant differences in A $\beta$ 42/40 and N-p-tau181 concentrations between the  
23 AD and other groups. Additionally, the AD group exhibited significantly higher  
24 mid-p-tau181 concentrations than did all other groups except the PSP group. Moreover,  
25 all disease groups had increased neurofilament light chain (NfL) concentrations  
26 compared to the CN group. ROC curve analyses (Figure 5B) revealed the following  
27 order of biomarkers according to their ability to discriminate between individuals with  
28 and without <sup>11</sup>C-PiB-PET-positive amyloid pathology when all participants were  
29 incorporated: N-p-tau181 (AUC = 0.867), A $\beta$ 42/40 (AUC = 0.850), mid-p-tau181  
30 (AUC = 0.771), and NfL (AUC = 0.555).

31

32 ***Trajectory analyses of imaging- and blood-based A/T/N biomarkers along with***  
33 ***cognitive decline in the CN and AD continuum subjects***

34 The imaging biomarkers examined in this cohort revealed that the A marker (i.e.,  
35 amyloid PET index) displayed a sigmoidal trajectory when plotted against cognitive  
36 deficits and reached a plateau when the MMSE score was around 20 points, the point at

1 which cognitive decline became apparent (Figure 6A). Conversely, the T marker (i.e.,  
2 tau PET index) displayed a linearly progressive increase with a decrease in the MMSE  
3 scores. The N marker (i.e., the volumetric MRI index) also tended to show a linear  
4 increment similar to that for the T marker, albeit with a lesser z-score range.

5 The blood-based biomarkers displayed trajectories closely resembling those of the  
6 imaging biomarkers, although their dynamic ranges were inferior to those of the  
7 imaging biomarkers (Figure 6B). Notably, the two different blood-based T markers  
8 showed clearly distinct trajectories such that plasma mid-p-tau181 levels exhibited a  
9 linearly progressive increase similar to the tau PET index with the decline in MMSE  
10 scores, whereas plasma N-p-tau181 levels measured using a currently widely used  
11 conventional p-tau assay (Quanterix) displayed a sigmoidal trajectory similar to that for  
12 amyloid PET with the decrease in MMSE scores. The A ( $A\beta_{42/40}$ ) and N (NfL)  
13 markers showed a sigmoidal curve and a linear progression, respectively, similar to  
14 those for the corresponding imaging biomarkers.

15

## 16 **Discussion**

17 The current study aimed to develop a novel plasma p-tau biomarker (mid-p-tau181) that  
18 could be potentially interchangeable with tau PET imaging and validate its ability to  
19 accurately reflect the extent of AD-type tau burden in the brain confirmed using tau PET.  
20 Notably, our results showed that the plasma mid-p-tau181 exhibited a strong correlation  
21 with the accumulation of tau PET ligands in AD brains and was accordingly able to  
22 discriminate positive and negative AD pathologies on tau PET. These findings indicate  
23 that plasma mid-p-tau levels could have sufficient accuracy in determining the existence  
24 of AD-type tau pathology in the brain without being affected by brain amyloid  
25 deposition, which has been known to affect the plasma levels of N-terminal to  
26 mid-domain forms of p-tau181 (N-p-tau) detected as plasma p-tau181 by most  
27 conventional p-tau assays.<sup>17,26</sup> Moreover, the trajectory of the change in the plasma  
28 levels of the mid-p-tau181 along with MMSE scores was similar to that observed with  
29 tau PET. These results strongly suggest the potential utility of plasma mid-p-tau181 as a  
30 blood-based biomarker for the detection and stratification of AD-type tau burden in the  
31 brain, mainly in the tau accumulation phase of the AD continuum.

32 Various experimental and clinical studies have suggested that an increase in soluble  
33 p-tau in biofluids could be strongly associated with  $A\beta$  aggregation.<sup>17,29,30,39-42</sup> This  
34 evidence indicates that tau hyperphosphorylation occurs in neurons exposed to  $A\beta$ , with  
35 p-tau levels increasing in response to  $A\beta$  deposition. Consistent with this notion, plasma  
36 p-tau is highly valuable for distinguishing AD from other neurodegenerative



1 diseases.<sup>18,43-45</sup> In addition, p-tau concentrations measured using conventional N-p-tau  
2 assays have been recognized as an early marker for AD given the increase in their  
3 values alongside A $\beta$  deposition<sup>17,44,46-49</sup> rather than before tau aggregation.<sup>19,28,30</sup>  
4 Meanwhile, the process of tangle maturation also needs to be considered when  
5 interpreting the levels of soluble p-tau in biofluids measured using immunoassay  
6 methodologies. Most current approaches for quantifying soluble p-tau via immunoassay  
7 predominantly target tau fragments phosphorylated at positions 181, 217, or 231 and  
8 bearing N-terminal epitopes.<sup>12</sup> The C-terminal portion of the tau protein, which is  
9 involved its aggregation,<sup>50</sup> is rarely present in soluble species of the tau protein. Thus,  
10 soluble tau fragments present in the body fluids usually include only the  
11 N-terminal-to-mid-region epitopes, ensuring consistent quantification using N-p-tau  
12 assays currently accessible.<sup>12</sup> Conversely, N-terminal cleavage also occurs in addition to  
13 its C-terminal cleavage in tau proteins insolubilized and deposited in the brain, which  
14 has been postulated to play a role in tangle evolution.<sup>33,51-53</sup> Therefore, this tau  
15 truncation implies that the accumulation of tau aggregates in the brain might not directly  
16 correspond with soluble p-tau quantified using conventional N-p-tau assays. Concurrent  
17 with this perspective, a study investigating the associations between various plasma  
18 p-tau species and amyloid/tau PET demonstrated that all plasma p-tau species measured  
19 by N-p-tau assays showed a considerably stronger correlation with amyloid PET  
20 binding than with tau PET binding.<sup>30</sup> These findings support the notion that currently  
21 available p-tau assays cannot be interchangeable with tau PET given that they do not  
22 accurately coincide with tau PET results and are also affected by amyloid deposition.  
23 Conversely, our mid-p-tau181 assay demonstrated a strong correlation with tau  
24 PET accumulation, but not with the amyloid PET ligand, in AD brains. The tau PET  
25 ligand employed in the current study, namely Florzorotau, exhibits high sensitivity to  
26 AD-specific tau lesions, including neurofibrillary tangles, neuropil threads, and neuritic  
27 plaques.<sup>34</sup> This suggests that our plasma mid-p-tau181, which is a previously  
28 nonexistent blood-based “T” biomarker in the ATN framework, corresponded to the  
29 AD-type tau accumulation in tau PET scans.  
30 Moreover, the characteristics of mid-p-tau181 suggest its usefulness as a biomarker  
31 for predicting the therapeutic response to current DMTs targeting A $\beta$ . These therapies  
32 are more likely to be effective when introduced before substantial tau aggregation.  
33<sup>2,11,54,55</sup> Therefore, identifying patients with high plasma mid-p-tau levels, in whom  
34 brain tau aggregation has been suggested to have progressed beyond the critical point,  
35 could help select patients more likely to benefit from DMTs targeting A $\beta$ , like so in the  
36 phase 3 study of donanemab.<sup>11</sup> Our results showed that our plasma mid-p-tau181 could

1 discriminate between tau-positive and -negative subjects with a specificity greater than  
2 85%, effectively excluding patients with advanced tau pathology.

3 Plasma mid-p-tau181 levels were also correlated with brain atrophy and increased  
4 with the progression of cognitive impairment evaluated using MMSE scores during  
5 trajectory analysis. Meanwhile, plasma N-p-tau181 levels increased in the early stage  
6 even when MMSE scores were within the normal range, and its increase slowed down  
7 in the later phase when cognitive impairment advanced. In support of these findings,  
8 CSF p-tau181 measured with an immunoassay targeting the mid-portion of tau protein  
9 also increased later than N-p-tau181,<sup>49</sup> as observed in our study. However, the increase  
10 in CSF N-p-tau181 species ceased and instead decreased after neuronal dysfunction  
11 started in the familial AD cohort.<sup>56</sup> Consequently, plasma mid-p-tau181 has been  
12 associated with the later stages of AD in contrast to N-p-tau181, which has been  
13 associated with the early stage just after amyloid deposition starts. Mid-p-tau181 could  
14 thus be utilized as a biomarker to monitor disease progression when cognitive  
15 impairment starts worsening due to tau accumulation in the brain.

16 The PSP group also showed a significant elevation in plasma mid-p-tau181,  
17 deviating from the results of the N-p-tau assay and leading to a slight decrease in  
18 specificity to AD. Phosphorylation in the mid-region has also been observed in non-AD  
19 tauopathies, such as PSP,<sup>57</sup> with some previous studies reporting that soluble p-tau  
20 levels in CSF might be elevated in non-AD tauopathies.<sup>58,59</sup> However, plasma  
21 mid-p-tau181 levels were not correlated with tau PET accumulation in the PSP patients  
22 (Supplementary Figure 8). Accordingly, the underlying pathophysiological basis for the  
23 observed increase in plasma mid-p-tau181 levels in our PSP group remains elusive.  
24 Although further investigations are still needed, plasma mid-p-tau181 might be a  
25 valuable biomarker for non-AD tauopathies.

26 This study has several limitations worth noting. Firstly, our sample size was  
27 modest, and longitudinal data was absent. As such, we are planning to conduct more  
28 studies in the near future to address these limitations. Secondly, we found that no  
29 correlation between the extent of amyloid burden in the brain evaluated through  
30 amyloid PET and not only plasma mid-p-tau181 levels but also N-p-tau181 levels in  
31 contrast to previous reports, which have shown a positive correlation between brain  
32 amyloid burden and plasma N-p-tau.<sup>26,30,32</sup> This discrepancy may be attributed to the  
33 demographics of the patients with AD continuum included in the current study, who  
34 predominantly comprise symptomatic AD cases and whose amyloid deposition in the  
35 brain has already plateaued. To confirm this phenomenon, we conducted correlation  
36 analyses between plasma p-tau181 levels and PET findings in the study participants,

1 including both the CN and AD continuum subjects (Supplementary Figure 9).  
2 Consistent with previous reports,<sup>30,32</sup> plasma N-p-tau181 levels were primarily  
3 correlated with amyloid PET results, whereas plasma mid-p-tau181 levels were  
4 correlated chiefly with tau PET results. Further validation of interactions between  
5 plasma p-tau species and amyloid/tau PET results are still required in independent  
6 cohorts, including very early AD cases, such as those with asymptomatic AD [A(+)]T(-)].  
7 Additional validation studies using alternative tau PET tracers, such as <sup>18</sup>F-MK6240,  
8 would certainly be informative. Moreover, although this study developed the  
9 mid-p-tau181 assay, the characteristics of plasma p-tau biomarkers, including which AD  
10 continuum stages a specific plasma p-tau molecule could reflect most, could vary  
11 depending on the phosphorylation site on the p-tau molecules.<sup>56,60</sup> Given some previous  
12 reports indicating a moderate correlation between p-tau217 and tau pathologies in the  
13 AD brain,<sup>18,19,32</sup> it is also intriguing to develop other assays targeting mid-p-tau species  
14 with phosphorylation sites other than 181.

15 Despite these limitations, the strength of the present study lies our development of  
16 an innovative mid-p-tau assay that corresponds with the AD-type brain tau burden  
17 determined using tau PET and its validation in a cohort of controls and AD continuum  
18 subjects who underwent both amyloid- and tau PET. Although specific assays have been  
19 reported to measure tau fragments in the CSF and exhibit correlations with brain tau  
20 pathologies,<sup>61,62</sup> there are still unmet needs for implementing comprehensively validated  
21 blood-based biomarkers that accurately reflect brain tau burden without being  
22 influenced by amyloid deposition. Our novel mid-p-tau assay is anticipated to function  
23 as a blood-based biomarker for the screening and monitoring of brain tau pathologies,  
24 especially in the selection of patients most suitable for anti-A $\beta$  DMTs and the  
25 development of tau-targeted therapies, although further longitudinal studies and  
26 validation in larger cohorts are necessary.

27

## 28 **Methods**

### 29 *Participants*

30 We recruited a cohort of 186 individuals comprising 43 CN individuals, 30 patients with  
31 MCI due to AD, 31 patients with dementia due to AD, 52 patients with PSP, and 30  
32 patients with other FTLD syndromes between January 2018 and September 2022. The  
33 other FTLDs comprised 12 cases with corticobasal syndrome (CBS), 10 cases with  
34 behavioral-variant frontotemporal dementia (BvFTD), 7 cases with frontotemporal  
35 dementia and parkinsonism linked to chromosome 17 MAPT (FTDP-17/MAPT), and 1  
36 case of primary progressive aphasia. CN individuals were those aged older than 40 years

1 who had no history of neurological and psychiatric disorders, had a MMSE score of  $\geq 28$ ,  
2 or had a Montreal Cognitive Assessment score of  $\geq 26$  and Geriatric Depression Scale  
3 score of  $\leq 5$ .<sup>35</sup> Patients with MCI and dementia due to AD underwent clinical evaluations.  
4 Cognitive impairment severity was defined as MMSE  $< 24$  and CDR  $\geq 1$  for dementia  
5 and MMSE  $\geq 26$  and CDR = 0.5 for MCI.<sup>35</sup> Patients with PSP and other FTLD  
6 syndromes were diagnosed according to established criteria previously reported.<sup>34,35</sup>

7 In the present study, the diagnosis of patients with MCI and dementia due to AD  
8 required brain amyloid positivity in PET scans, and they were combined and categorized  
9 into the AD group based on the concept of the AD continuum. We excluded patients with  
10 PSP and other FTLD who had positive amyloid PET results to eliminate the influence of  
11 mixed pathology. Those with other FTLDs were heterogeneous and categorized into the  
12 FTLD group. Furthermore, CN individuals with a positive result on either or both  
13 amyloid and tau PET scans were also excluded as they were considered to have been in  
14 the preclinical AD stage. Amyloid positivity was defined based on <sup>11</sup>C-PiB-PET visual  
15 inspection performed by a minimum of three specialists with expertise in the field.<sup>34</sup> Tau  
16 PET negativity in CN individuals was defined according to the AD tau score ( $< 0.1986$ )  
17 and PSP tau score ( $< 0.3431$ ) as reported previously.<sup>35</sup> These scores, which were  
18 calculated from <sup>18</sup>F-florzorotau PET images via our established machine learning  
19 algorithm, possess a high degree of sensitivity and specificity in discriminating CN  
20 individuals from patients with AD and PSP.<sup>35</sup> Consequently, after excluding 3 CN  
21 individuals and 11 MCI, 2 AD, 2 PSP, and 4 FTLD patients according to the  
22 aforementioned criteria, our final cohort consisted of 164 participants comprising 40 CN  
23 individuals and 48 AD, 50 PSP, and 26 FTLD patients.

24 This study was approved by the National Institutes for Quantum Science and  
25 Technology Certified Review Board. Written informed consent was obtained from all  
26 participants and spouses or close family members when participants were cognitively  
27 impaired. This study was registered with the UMIN Clinical Trial Registry  
28 (UMIN-CRT; number 000041383).

29

### 30 ***Blood sampling***

31 We obtained blood samples through venous puncture on the same day as the PET scan. A  
32 total of 8 mL of blood was collected in ethylenediaminetetraacetic acid  
33 (EDTA)-containing tubes. After collection, plasma was separated by centrifugation for 10  
34 min at 2000g, aliquoted into polypropylene tubes, and then stored at  $-80^{\circ}\text{C}$  until analysis.

35

### 36 ***Measurements of blood biomarkers***

1 We developed a novel immunoassay able to quantify plasma levels of both N- and  
2 C-terminally truncated p-tau181 fragments run on a highly sensitive automated digital  
3 ELISA platform (Simoa HD-X Analyzer, Quanterix, Lexington, KY, USA) and measured  
4 the levels of p-tau181 including such fragments in human plasma. The details of the  
5 procedures for method validation of this original immunoassay are described in the  
6 Supplementary Methods and Results. We also quantified plasma levels of the A/T/N  
7 biomarkers<sup>7</sup> (A $\beta$ 42, A $\beta$ 40, p-tau181, and NfL instead of total tau in the original paper)  
8 utilizing the Simoa platform (Quanterix) equipped with validated assay kits. Procedures  
9 were performed following the manufacturer's instructions. This study employed the  
10 A $\beta$ 42/A $\beta$ 40 ratio as a proxy for cerebral amyloid burden. Plasma p-tau181 measured  
11 using the commercial kit (Simoa pTau-181 V2.1 Assay, Quanterix) was defined as  
12 N-p-tau181, whereas plasma p-tau181 measured using the originally developed  
13 immunoassay run on the Simoa system was defined as mid-p-tau181.

14 All plasma samples were diluted four times with the respective sample diluent  
15 before the assays to minimize matrix effects. All plasma samples were run in duplicate  
16 with the same lot of standards. The relative concentration estimates of plasma biomarkers  
17 were calculated according to their respective standard curves.

18

### 19 ***PET and MRI data acquisition***

20 Amyloid and tau deposits in the brains of all participants were assessed using PET with  
21 <sup>11</sup>C-PiB and <sup>18</sup>F-florzorotau as described in other clinical trials (UMIN-CRT; number  
22 000026385, 000026490, 000029608, 000030248, and 000043458). One PSP patient who  
23 had already been confirmed to be A $\beta$ -negative at another facility no longer underwent  
24 <sup>11</sup>C-PiB-PET at our center. The scan protocol was described as follows: parametric  
25 <sup>11</sup>C-PiB-PET images were acquired 50–70 min after injection (injected dose:  $528.5 \pm 65.5$   
26 MBq, molar activity  $90.2 \pm 26.2$  GBq/ $\mu$ mol); <sup>18</sup>F-florzorotau PET images were obtained  
27 90–110 min after injection (injected dose:  $186.6 \pm 7.4$  MBq, molar activity  $244.2 \pm 86.7$   
28 GBq/ $\mu$ mol). PET was primarily conducted using a Biograph mCT flow system (Siemens  
29 Healthcare), with some cases using the Discovery MI (GE Healthcare) (9 <sup>11</sup>C-PiB scans  
30 in CN individuals; 22 <sup>11</sup>C-PiB scans and 3 <sup>18</sup>F-florzorotau scans in AD patients; 7 <sup>11</sup>C-PiB  
31 scans in PSP patients; and 4 <sup>11</sup>C-PiB scans in FTLD patients) and an ECAT EXACT HR+  
32 scanner (CTI PET Systems, Inc.) (three <sup>11</sup>C-PiB scans in CN individuals, four <sup>11</sup>C-PiB  
33 scans in AD patients, nine <sup>11</sup>C-PiB scans in PSP patients, and three <sup>11</sup>C-PiB scans in  
34 FTLD patients). Acquired PET images were reconstructed using the filtered back  
35 projection method with a Hanning filter. MRI examination was conducted simultaneously  
36 with PET using a 3-T scanner (MAGNETOM Verio; Siemens Healthcare). The

1 anatomical images were acquired using a three-dimensional T1-weighted gradient echo  
2 sequence that produced a gapless series of thin sagittal sections (TE = 1.95 ms, TR = 2300  
3 ms, TI = 900 ms, flip angle = 9°, acquisition matrix = 512 × 512 × 176, voxel size = 1 ×  
4 0.488 × 0.488 mm<sup>3</sup>).

5

### 6 ***Imaging analyses***

7 All images were preprocessed using PMOD software (version 4.3, PMOD Technologies  
8 Ltd), FreeSurfer 6.0 (<http://surfer.nmr.mgh.harvard.edu/>), MATLAB (The Mathworks,  
9 Natick, MA, USA), and Statistical Parametric Mapping software (SPM12, Wellcome  
10 Department of Cognitive Neurology). PET images were co-registered with individual  
11 anatomical T1-weighted MR images, and SUVR images were generated using each  
12 reference region. The cerebellar cortex was the reference region for the <sup>11</sup>C-PiB-PET  
13 images. For <sup>18</sup>F-florzorotau PET images, an optimized reference region was set through  
14 an in-house MATLAB script that considered the distribution of diverse tau lesions  
15 throughout the entire gray matter and extracted optimized reference regions on an  
16 individual basis.<sup>63</sup> Each PET and MR image was also normalized to the Montreal  
17 Neurologic Institute space using the Diffeomorphic Anatomical Registration Through  
18 Exponentiated Lie Algebra (DARTEL) algorithm and was smoothed with a Gaussian  
19 kernel at 8-mm full-width at half maximum in voxel-wise analyses.

20 We performed an ROI analysis targeting AD pathologies on each imaging modality  
21 to quantify the regional amyloid/tau burden and cortical thinning. The amyloid burden  
22 was assessed using a Centiloid atlas (frontal, temporal, parietal, precuneus, anterior  
23 striatum, and insula) implemented in the PMOD Neuro Tool (PMOD Technologies Ltd).  
24 Each Centiloid SUVR was calculated and converted to a Centiloid score (CL score)<sup>64</sup>  
25 using PET data from 12 young CN individuals aged 23–43 years and 25 cases of AD  
26 patients scanned at our institution. Tau burden was assessed using ROIs targeting tau  
27 pathology associated with AD labeling through FreeSurfer, Braak staging ROIs (I/II,  
28 III/IV, V/VI),<sup>36</sup> and temporal meta-ROI (entorhinal, amygdala, parahippocampal,  
29 fusiform, inferior temporal, and middle temporal).<sup>37</sup> We excluded the hippocampus from  
30 the Braak stage I/II ROI because of potential spill-in from the choroid plexus.<sup>34</sup>  
31 Additionally, we also estimated the AD tau score to assess AD-type tau burden in the  
32 brain, which was calculated using an Elastic Net model trained on tau PET data as  
33 previously reported.<sup>35</sup> A qualitative analysis based on the values obtained from these  
34 ROI analyses was also conducted to evaluate the presence of tau lesions. For Braak  
35 staging, the SUVR values were converted to z-values based on another young CN  
36 cohort, and the highest stage was assigned based on the average regional Z-score (>2.5).

1 Those with stages 0–I/II were classified as tau-negative, whereas those with stages  
2 III/IV–V/VI were classified as tau-positive. The cutoff value of temporal meta-ROI  
3 SUVR was set at 1.105 to maximize the differentiation between CN individuals and AD  
4 patients during ROC analysis (see Supplementary material for detailed information).  
5 and the cutoff value of AD tau score was set at 0.1986 as described elsewhere.<sup>35</sup>  
6 Cortical thickness was measured using the cortical signature of AD through FreeSurfer  
7 (medial temporal, inferior temporal, temporal pole, angular, superior frontal, superior  
8 parietal, supramarginal, precuneus, and middle frontal).<sup>38</sup>

### 9 10 ***Statistical analyses***

11 Statistical analyses were conducted using GraphPad Prism version 9 (GraphPad  
12 Software). Initially, group comparisons were performed using the Kruskal–Wallis test or  
13 Mann–Whitney U test for demographic data and measured blood biomarker values and  
14 Fisher's exact test for gender ( $p < 0.05$ , corrected by Dunn's multiple comparisons).  
15 Subsequently, correlation analyses were conducted to verify the association between each  
16 p-tau181 assay and each imaging biomarker. During voxel-based analyses, a linear  
17 regression model was applied using SPM12. The extent threshold was established based  
18 on the expected voxels per cluster. For multiple voxel comparisons, family-wise error  
19 corrections at the cluster level were applied ( $p < 0.05$ , FWE-corrected). During  
20 ROI-based analyses, Pearson's correlation analyses were performed ( $p < 0.05$ , corrected  
21 by Bonferroni multiple comparisons), and nonlinear regression analysis (quadratic) was  
22 conducted when no significant correlation was observed. Results were adopted when the  
23 nonlinear analysis based on Akaike's Information Criterion (AIC) showed a better fit than  
24 the linear one. In addition, ability of each blood biomarker to discriminate between the  
25 presence or absence of AD pathology, as defined by amyloid or tau PET positivity, was  
26 also evaluated by calculating AUC values from ROC curve analyses. The Youden index  
27 maximizing sensitivity plus specificity minus one determined the optimized cutoff value.  
28 Finally, to explore the trajectories from CN to AD for each blood/imaging biomarker, we  
29 converted each biomarker value to a z-value based on CN data. Thereafter, we examined  
30 their relationship with cognitive dysfunction (MMSE score). A linear or sigmoidal 4PL  
31 regression analysis was adapted, and the better-fitting model was selected based on AIC.

### 32 33 **Data availability**

34 The data supporting this study's findings are available from the corresponding author on  
35 reasonable request. Sharing and reuse of data require the expressed written permission  
36 of the authors, as well as clearance from the Institutional Review Boards.

1

2 **References**

- 3 1. Nichols, E. *et al.* Estimation of the global prevalence of dementia in 2019 and  
4 forecasted prevalence in 2050: an analysis for the Global Burden of Disease Study  
5 2019. *The Lancet Public Health* **7**, e105–e125 (2022).
- 6 2. Cummings, J. *et al.* Alzheimer’s disease drug development pipeline: 2022.  
7 *Alzheimers Dement. (N. Y.)* **8**, e12295 (2022).
- 8 3. EMERGE and EMERGE and ENGAGE Topline Results: Two Phase 3 Studies to  
9 Evaluate Aducanumab in Patients With Early Alzheimer’s Disease  
10 (<https://investors.biogen.com/static-files/ddd45672-9c7e-4c99-8a06-3b557697c06f>).  
11 2019.
- 12 4. Sims, J. R. *et al.* Donanemab in early symptomatic Alzheimer disease: The  
13 TRAILBLAZER-ALZ 2 randomized clinical trial. *JAMA* **330**, 512–527 (2023).
- 14 5. van Dyck, C. H. *et al.* Lecanemab in early Alzheimer’s disease. *N. Engl. J. Med.*  
15 **388**, 9–21 (2023).
- 16 6. Imbimbo, B. P., Ippati, S., Watling, M. & Balducci, C. A critical appraisal of  
17 tau-targeting therapies for primary and secondary tauopathies. *Alzheimers. Dement.*  
18 **18**, 1008–1037 (2022).
- 19 7. Jack, C. R., Jr *et al.* NIA-AA Research Framework: Toward a biological definition  
20 of Alzheimer’s disease. *Alzheimers. Dement.* **14**, 535–562 (2018).
- 21 8. Villemagne, V. L., Doré, V., Burnham, S. C., Masters, C. L. & Rowe, C. C. Imaging  
22 tau and amyloid- $\beta$  proteinopathies in Alzheimer disease and other conditions. *Nat.*  
23 *Rev. Neurol.* **14**, 225–236 (2018).
- 24 9. Teng, E. *et al.* Safety and efficacy of semorinemab in individuals with prodromal to  
25 mild Alzheimer disease: A randomized clinical trial. *JAMA Neurol.* **79**, 758–767  
26 (2022).
- 27 10. Sevigny, J. *et al.* The antibody aducanumab reduces A $\beta$  plaques in Alzheimer’s  
28 disease. *Nature* **537**, 50–56 (2016).
- 29 11. Mintun, M. A., Wessels, A. M. & Sims, J. R. Donanemab in early Alzheimer’s  
30 disease. Reply. *The New England journal of medicine* vol. 385 667 (2021).
- 31 12. Karikari, T. K. *et al.* Blood phospho-tau in Alzheimer disease: analysis,  
32 interpretation, and clinical utility. *Nat. Rev. Neurol.* **18**, 400–418 (2022).
- 33 13. Dubois, B. *et al.* Advancing research diagnostic criteria for Alzheimer’s disease: the  
34 IWG-2 criteria. *Lancet Neurol.* **13**, 614–629 (2014).
- 35 14. McKhann, G. M. *et al.* The diagnosis of dementia due to Alzheimer’s disease:  
36 recommendations from the National Institute on Aging-Alzheimer’s Association



- 1 workgroups on diagnostic guidelines for Alzheimer's disease. *Alzheimers. Dement.*
- 2 **7**, 263–269 (2011).
- 3 15. Hansson, O. *et al.* The Alzheimer's association appropriate use recommendations
- 4 for blood biomarkers in Alzheimer's disease. *Alzheimers. Dement.* **18**, (2022).
- 5 16. Tatebe, H. *et al.* Quantification of plasma phosphorylated tau to use as a biomarker
- 6 for brain Alzheimer pathology: pilot case-control studies including patients with
- 7 Alzheimer's disease and down syndrome. *Mol. Neurodegener.* **12**, 63 (2017).
- 8 17. Karikari, T. K. *et al.* Blood phosphorylated tau 181 as a biomarker for Alzheimer's
- 9 disease: a diagnostic performance and prediction modelling study using data from
- 10 four prospective cohorts. *Lancet Neurol.* **19**, 422–433 (2020).
- 11 18. Palmqvist, S. *et al.* Discriminative accuracy of plasma phospho-tau217 for
- 12 Alzheimer disease vs other neurodegenerative disorders. *JAMA* **324**, 772–781
- 13 (2020).
- 14 19. Janelidze, S. *et al.* Associations of Plasma Phospho-Tau217 Levels With Tau
- 15 Positron Emission Tomography in Early Alzheimer Disease. *JAMA Neurol.* **78**,
- 16 149–156 (2021).
- 17 20. Fitzpatrick, A. W. P. *et al.* Cryo-EM structures of tau filaments from Alzheimer's
- 18 disease. *Nature* **547**, 185–190 (2017).
- 19 21. Koss, D. J. *et al.* Soluble pre-fibrillar tau and  $\beta$ -amyloid species emerge in early
- 20 human Alzheimer's disease and track disease progression and cognitive decline.
- 21 *Acta Neuropathol.* **132**, 875–895 (2016).
- 22 22. Han, P. *et al.* A Quantitative Analysis of Brain Soluble Tau and the Tau Secretion
- 23 Factor. *J. Neuropathol. Exp. Neurol.* **76**, 44–51 (2017).
- 24 23. Sato, C. *et al.* Tau Kinetics in Neurons and the Human Central Nervous System.
- 25 *Neuron* **98**, 861–864 (2018).
- 26 24. Thijssen, E. H. *et al.* Diagnostic value of plasma phosphorylated tau181 in
- 27 Alzheimer's disease and frontotemporal lobar degeneration. *Nat. Med.* **26**, 387–397
- 28 (2020).
- 29 25. Lantero Rodriguez, J. *et al.* Plasma p-tau181 accurately predicts Alzheimer's
- 30 disease pathology at least 8 years prior to post-mortem and improves the clinical
- 31 characterisation of cognitive decline. *Acta Neuropathol.* **140**, 267–278 (2020).
- 32 26. Karikari, T. K. *et al.* Diagnostic performance and prediction of clinical progression
- 33 of plasma phospho-tau181 in the Alzheimer's Disease Neuroimaging Initiative. *Mol.*
- 34 *Psychiatry* **26**, 429–442 (2021).
- 35 27. Palmqvist, S. *et al.* Prediction of future Alzheimer's disease dementia using plasma
- 36 phospho-tau combined with other accessible measures. *Nat. Med.* **27**, 1034–1042

- 1 (2021).
- 2 28. Groot, C. *et al.* Phospho-tau with subthreshold tau-PET predicts increased tau  
3 accumulation rates in amyloid-positive individuals. *Brain* (2022)  
4 doi:10.1093/brain/awac329.
- 5 29. Mattsson-Carlgen, N. *et al.* Soluble P-tau217 reflects amyloid and tau pathology  
6 and mediates the association of amyloid with tau. *EMBO Mol. Med.* **13**, e14022  
7 (2021).
- 8 30. Therriault, J. *et al.* Association of Phosphorylated Tau Biomarkers With Amyloid  
9 Positron Emission Tomography vs Tau Positron Emission Tomography. *JAMA*  
10 *Neurol.* (2022) doi:10.1001/jamaneurol.2022.4485.
- 11 31. Smirnov, D. S. *et al.* Plasma biomarkers for Alzheimer’s Disease in relation to  
12 neuropathology and cognitive change. *Acta Neuropathol.* **143**, 487–503 (2022).
- 13 32. Salvadó, G. *et al.* Specific associations between plasma biomarkers and  
14 postmortem amyloid plaque and tau tangle loads. *EMBO Mol. Med.* e2463 (2023).
- 15 33. Guillozet-Bongaarts, A. L. *et al.* Tau truncation during neurofibrillary tangle  
16 evolution in Alzheimer’s disease. *Neurobiol. Aging* **26**, 1015–1022 (2005).
- 17 34. Tagai, K. *et al.* High-Contrast In Vivo Imaging of Tau Pathologies in Alzheimer’s  
18 and Non-Alzheimer’s Disease Tauopathies. *Neuron* **109**, 42-58.e8 (2021).
- 19 35. Endo, H. *et al.* A Machine Learning-Based Approach to Discrimination of  
20 Tauopathies Using [18 F]PM-PBB3 PET Images. *Mov. Disord.* **37**, 2236–2246  
21 (2022).
- 22 36. Schöll, M. *et al.* PET Imaging of Tau Deposition in the Aging Human Brain.  
23 *Neuron* **89**, 971–982 (2016).
- 24 37. Ossenkoppele, R. *et al.* Discriminative Accuracy of [18F]flortaucipir Positron  
25 Emission Tomography for Alzheimer Disease vs Other Neurodegenerative  
26 Disorders. *JAMA* **320**, 1151–1162 (2018).
- 27 38. Dickerson, B. C. *et al.* The Cortical Signature of Alzheimer’s Disease: Regionally  
28 Specific Cortical Thinning Relates to Symptom Severity in Very Mild to Mild AD  
29 Dementia and is Detectable in Asymptomatic Amyloid-Positive Individuals. *Cereb.*  
30 *Cortex* **19**, 497–510 (2008).
- 31 39. Venkatramani, A. & Panda, D. Regulation of neuronal microtubule dynamics by  
32 tau: Implications for tauopathies. *Int. J. Biol. Macromol.* **133**, 473–483 (2019).
- 33 40. Zhang, F. *et al.*  $\beta$ -amyloid redirects norepinephrine signaling to activate the  
34 pathogenic GSK3 $\beta$ /tau cascade. *Sci. Transl. Med.* **12**, (2020).
- 35 41. He, Z. *et al.* Amyloid- $\beta$  plaques enhance Alzheimer’s brain tau-seeded pathologies  
36 by facilitating neuritic plaque tau aggregation. *Nat. Med.* **24**, 29–38 (2018).

- 1 42. Maia, L. F. *et al.* Changes in amyloid- $\beta$  and Tau in the cerebrospinal fluid of  
2 transgenic mice overexpressing amyloid precursor protein. *Sci. Transl. Med.* **5**,  
3 194re2 (2013).
- 4 43. Karikari, T. K. *et al.* Diagnostic performance and prediction of clinical progression  
5 of plasma phospho-tau181 in the Alzheimer's Disease Neuroimaging Initiative.  
6 *bioRxiv* (2020) doi:10.1101/2020.07.15.20154237.
- 7 44. Thijssen, E. H. *et al.* Plasma phosphorylated tau 217 and phosphorylated tau 181 as  
8 biomarkers in Alzheimer's disease and frontotemporal lobar degeneration: a  
9 retrospective diagnostic performance study. *Lancet Neurol.* **20**, 739–752 (2021).
- 10 45. Benussi, A. *et al.* Classification accuracy of blood-based and neurophysiological  
11 markers in the differential diagnosis of Alzheimer's disease and frontotemporal  
12 lobar degeneration. *Alzheimers. Res. Ther.* **14**, 155 (2022).
- 13 46. Mielke, M. M. *et al.* Comparison of Plasma Phosphorylated Tau Species With  
14 Amyloid and Tau Positron Emission Tomography, Neurodegeneration, Vascular  
15 Pathology, and Cognitive Outcomes. *JAMA Neurol.* **78**, 1108–1117 (2021).
- 16 47. Janelidze, S. *et al.* Head-to-head comparison of 10 plasma phospho-tau assays in  
17 prodromal Alzheimer's disease. *Brain* (2022) doi:10.1093/brain/awac333.
- 18 48. Milà-Alomà, M. *et al.* Plasma p-tau231 and p-tau217 as state markers of amyloid- $\beta$   
19 pathology in preclinical Alzheimer's disease. *Nat. Med.* **28**, 1797–1801 (2022).
- 20 49. Suárez-Calvet, M. *et al.* Novel tau biomarkers phosphorylated at T181, T217 or  
21 T231 rise in the initial stages of the preclinical Alzheimer's continuum when only  
22 subtle changes in A $\beta$  pathology are detected. *EMBO Mol. Med.* **12**, e12921 (2020).
- 23 50. Dujardin, S. *et al.* Tau molecular diversity contributes to clinical heterogeneity in  
24 Alzheimer's disease. *Nat. Med.* **26**, 1256–1263 (2020).
- 25 51. García-Sierra, F., Ghoshal, N., Quinn, B., Berry, R. W. & Binder, L. I.  
26 Conformational changes and truncation of tau protein during tangle evolution in  
27 Alzheimer's disease. *J. Alzheimers. Dis.* **5**, 65–77 (2003).
- 28 52. Bondareff, W. *et al.* Molecular analysis of neurofibrillary degeneration in  
29 Alzheimer's disease. An immunohistochemical study. *Am. J. Pathol.* **137**, 711–723  
30 (1990).
- 31 53. Horowitz, P. M. *et al.* Early N-terminal changes and caspase-6 cleavage of tau in  
32 Alzheimer's disease. *J. Neurosci.* **24**, 7895–7902 (2004).
- 33 54. Bloom, G. S. Amyloid- $\beta$  and tau: the trigger and bullet in Alzheimer disease  
34 pathogenesis. *JAMA Neurol.* **71**, 505–508 (2014).
- 35 55. Cai, Y. *et al.* Initial levels of  $\beta$ -amyloid and tau deposition have distinct effects on  
36 longitudinal tau accumulation in Alzheimer's disease. *Alzheimers. Res. Ther.* **15**, 30

- 1 (2023).
- 2 56. Barthélemy, N. R. *et al.* A soluble phosphorylated tau signature links tau, amyloid  
3 and the evolution of stages of dominantly inherited Alzheimer’s disease. *Nat. Med.*  
4 **26**, 398–407 (2020).
- 5 57. Kametani, F. *et al.* Comparison of Common and Disease-Specific Post-translational  
6 Modifications of Pathological Tau Associated With a Wide Range of Tauopathies.  
7 *Front. Neurosci.* **14**, 581936 (2020).
- 8 58. Sato, C. *et al.* MAPT R406W increases tau T217 phosphorylation in absence of  
9 amyloid pathology. *Ann Clin Transl Neurol* **8**, 1817–1830 (2021).
- 10 59. Kurihara, M. *et al.* CSF P-Tau181 and Other Biomarkers in Patients With Neuronal  
11 Intranuclear Inclusion Disease. *Neurology* **100**, e1009–e1019 (2023).
- 12 60. Barthélemy, N. R. *et al.* Cerebrospinal fluid phospho-tau T217 outperforms T181 as  
13 a biomarker for the differential diagnosis of Alzheimer’s disease and PET  
14 amyloid-positive patient identification. *Alzheimers. Res. Ther.* **12**, 26 (2020).
- 15 61. Blennow, K. *et al.* Cerebrospinal fluid tau fragment correlates with tau PET: a  
16 candidate biomarker for tangle pathology. *Brain* **143**, 650–660 (2020).
- 17 62. Horie, K. *et al.* CSF MTBR-tau243 is a specific biomarker of tau tangle pathology  
18 in Alzheimer’s disease. *Nat. Med.* **29**, 1954–1963 (2023).
- 19 63. Tagai, K. *et al.* An optimized reference tissue method for quantification of tau  
20 protein depositions in diverse neurodegenerative disorders by PET with  
21 18F-PM-PBB3 (18F-APN-1607). *Neuroimage* **264**, 119763 (2022).
- 22 64. Klunk, W. E. *et al.* The Centiloid Project: Standardizing quantitative amyloid  
23 plaque estimation by PET. *Alzheimers. Dement.* **11**, 1 (2015).

24

## 25 **Funding**

26 This study was supported in part by AMED under Grant Numbers JP18dm0207018,  
27 JP19dm0207072, JP18dk0207026, JP19dk0207049, 21wm0425015h0001, and  
28 20356533; MEXT KAKENHI under Grant Numbers JP16H05324 and JP18K07543;  
29 JST under Grant Numbers JPMJCR1652 and JPMJMS2024; and the Kao Research  
30 Council for the Study of Healthcare Science, Biogen Idec Inc. and APRINOIA  
31 Therapeutics.

32

## 33 **Acknowledgements**

34 The authors thank all patients and their caregivers for participation in this study, as  
35 well as clinical research coordinators, PET and MRI operators, radiochemists, and  
36 research ethics advisers at QST for their assistance with the current projects. We thank

1 APRINOIA Therapeutics for kindly sharing a precursor of <sup>18</sup>F-florzorotau. The authors  
2 acknowledge support with the recruitment of patients by Shunichiro Shinagawa at the  
3 Department of Psychiatry, Jikei University School of Medicine; Shigeki Hirano at the  
4 Department of Neurology, Chiba University; Taku Hatano, Yumiko Motoi, and Shinji  
5 Saiki at the Department of Neurology, Juntendo University School of Medicine; Ikuko  
6 Aiba at the Department of Neurology, National Hospital Organization Higashinagoya  
7 National Hospital; Yasushi Shiio and Tomonari Seki at the Department of Neurology,  
8 Tokyo Teishin Hospital; Hisaomi Suzuki at the National Hospital Organization  
9 Shimofusa Psychiatric Medical Center.

10

#### 11 **Author contributions**

12 **Kenji Tagai, Harutsugu Tatebe:** Conceptualization, Methodology, Formal  
13 analysis, Writing - original draft. **Sayo Matsuura, Zhang Hong:** Measurement of  
14 samples. **Naomi Kokubo, Kiwamu Matsuoka, Hironobu Endo, Asaka Oyama,**  
15 **Kosei Hirata, Hitoshi Shinotoh, Yuko Kataoka, Hideki Matsumoto, Masaki Oya,**  
16 **Shin Kurose, Keisuke Takahata, Masanori Ichihashi, Manabu Kubota, Chie Seki,**  
17 **Hitoshi Shimada, Yuhei Takado:** Collection of clinical data. **Kazunori Kawamura,**  
18 **Ming-Rong Zhang:** Radioligand synthesis. **Yoshiyuki Soeda, Akihiko Takashima:**  
19 Assay validation. **Makoto Higuchi, Takahiko Tokuda:** Conceptualization, Writing -  
20 review & editing, Funding acquisition, Supervision

21

#### 22 **Competing interests**

23 Hitoshi Shimada, Ming-Rong Zhang, and Makoto Higuchi hold patents on  
24 compounds related to the present report (JP 5422782/EP 12 884  
25 742.3/CA2894994/HK1208672).

26

1 **Table 1.** Demographic and blood biomarker data of the participants.

2

	CN	AD	PSP	FTLD
Demographics				
Number	40	48	50	26
Age	66.0 (10.4)	69.3 (11.4)	71.2 (7.5)	65.0 (11.4)
Gender (male/female)	21/19	27/21	21/29	18/8
Years of schooling	14.8 (1.6)	13.9 (2.2)	13.6 (2.6)	14.0 (2.8)
MMSE	29.3 (1.0) <sup>†</sup>	21.9 (4.1) <sup>*</sup>	24.8 (5.8) <sup>*†</sup>	23.8 (6.1) <sup>*</sup>
FAB	16.7 (1.2) <sup>†</sup>	13.0 (3.0) <sup>*</sup>	12.0 (3.6) <sup>*</sup>	11.0 (4.8) <sup>*</sup>
CDR (0.5/1/2/3)	N/A	23/20/4/1	N/A	N/A
PSPRS	N/A	N/A	38.1 (18.2)	N/A
Blood biomarkers				
Aβ42/40	0.093 (0.020) <sup>†</sup>	0.067 (0.020) <sup>†</sup>	0.096 (0.048) <sup>†</sup>	0.089 (0.022) <sup>†</sup>
N-p-tau181 (pg/mL)	1.82 (0.79) <sup>†</sup>	4.07 (1.52) <sup>*</sup>	2.27 (1.06) <sup>†</sup>	2.25 (1.25) <sup>†</sup>
mid-p-tau181 (pg/mL)	0.83 (0.65) <sup>†</sup>	2.30 (1.31) <sup>*</sup>	1.56 (0.91) <sup>*</sup>	0.96 (0.63) <sup>†</sup>
NfL (pg/mL)	19.5 (12.5) <sup>†‡</sup>	33.2 (21.3) <sup>*‡</sup>	58.3 (39.7) <sup>*†</sup>	51.8 (39.3) <sup>*</sup>

3 CN, cognitively normal; AD, Alzheimer's disease; PSP, progressive supranuclear palsy;  
4 FTLD, frontotemporal degeneration; MMSE, Mini-Mental State Examination; FAB,  
5 Frontal Assessment Battery; CDR, Clinical Dementia Rating scale; PSPRS, progressive  
6 supranuclear palsy rating scale; N/A, not applicable; Aβ, amyloid beta; N-p-tau181,  
7 phosphorylated tau181 measured using the commercial kit directed to the C-terminally  
8 truncated N-terminal fragment of p-tau (Simoa pTau-181 V2.1 Assay, Quanterix);  
9 mid-p-tau181, phosphorylated tau181 measured using the originally developed  
10 immunoassay directed to both the N- and C-terminally truncated p-tau181 fragments;  
11 NfL, neurofilament light chain.

12 Values are presented as mean ± standard deviation.

13 <sup>\*</sup>, Significant difference between CN, <sup>†</sup>, between AD, <sup>‡</sup>, between PSP,  $P < 0.05$   
14 (corrected by Dunn's multiple comparisons)

15

1 **Table 2.** Performance of mid-p-tau181 in discriminating tau PET status determined  
2 using three different methods of evaluating brain tau burden on tau PET in the  
3 cognitively normal and AD continuum subjects

4

	Sensitivity (%)	Specificity (%)	Cutoff value (pg/mL)	AUC
Braak staging	62.8	92.5	1.76	0.859
Temporal meta SUVR	71.8	88.6	1.69	0.855
AD tau score	70.5	88.1	1.62	0.870

5

6 All parameters were estimated from receiver operating characteristic curve analyses. We  
7 set each cutoff value according to Youden index obtained in the respective receiver  
8 operating characteristic analyses.

9 SUVR, standardized uptake value ratio; AUC, area under the receiver operating  
10 characteristic curve.

11

12

1 **Figure legends**

2

3 **Figure 1. Correlations between plasma mid-p-tau levels and tau PET results in the**  
4 **subjects with AD continuum.**

5 (A) The correlation between plasma mid-p-tau181 levels and <sup>18</sup>F-florzorotau tau PET is  
6 depicted through its topographical representation ( $p < 0.05$ , family-wise error  
7 corrected).

8 (B, C) The correlation between plasma mid-p-tau181 levels and tau PET tracer  
9 accumulation in each ROI is portrayed via scatter plots. Pearson's correlation analysis  
10 was employed to calculate the  $r$  and  $p$  values. Statistical significance was established at  
11  $p < 0.0125$ , corrected for multiple comparisons using the Bonferroni method based on  
12 the number of ROIs. Regression analysis, indicated by a straight or curved line, depicts  
13 the preferred model, with its goodness of fit quantified using the  $R^2$  value.

14 SUVR, standardized uptake value ratio; AD tau score, a machine learning-based  
15 measure indicating AD-related features in tau PET images.

16 Mid-p-tau181, phosphorylated tau181 measured using the originally developed  
17 immunoassay directed to both N- and C-terminally truncated p-tau181 fragments.

18

19 **Figure 2 Correlation between plasma N-p-tau levels measured using a conventional**  
20 **p-tau assay and tau PET results in the subjects with AD continuum.**

21 (A) The correlation between plasma N-p-tau181 levels and tau PET results is  
22 demonstrated through its topographical representation ( $p < 0.05$ , uncorrected).

23 (B, C) The correlation between plasma N-p-tau181 levels and tau PET tracer  
24 accumulation in each ROI is depicted via scatter plots. Pearson's correlation analysis  
25 was utilized to calculate the  $r$  and  $p$  values. The preferred model, indicated by regression  
26 analysis, is depicted by a straight or curved line, with its goodness of fit quantified using  
27 the  $R^2$  value.

28 SUVR, standardized uptake value ratio; AD tau score, a machine learning-based  
29 measure indicating AD-related features in tau PET images.

30 N-p-tau181, phosphorylated tau181 measured using the Simoa pTau-181 V2.1 Assay kit  
31 (Quanterix).

32

33 **Figure 3. Scatter plots and ROC curves of the mid-p-tau181 showing its ability to**  
34 **discriminate between tau PET statuses determined by three different approaches**  
35 **in the cognitively normal and AD continuum subjects.**



1 Scatterplots (A) and ROC curves (B) illustrating the relationship between mid-p-tau181  
2 levels and positive/negative tau PET results as determined by three different methods. In  
3 the scatterplot, CN subjects are represented in purple, whereas AD continuum patients  
4 are depicted in blue. The dotted line represents the mid-p-tau181 cutoff calculated based  
5 on each approach.  $p < 0.0001$  (\*\*\*\*), as assessed by Mann–Whitney U test.

6

7 **Figure 4. Correlations between plasma mid-p-tau and N-p-tau levels and MRI**  
8 **structural images in the subjects with AD continuum.**

9 (A) The correlation between p-tau181 measured using the mid-p-tau181 or N-p-tau  
10 assay and brain atrophy is depicted through its topographical representation ( $p < 0.05$ ,  
11 uncorrected).

12 (B) The correlation between plasma mid-p-tau181 and N-p-tau levels measured using  
13 each assay and the thinning of the AD cortical signature is demonstrated via scatter  
14 plots. Pearson's correlation analysis was utilized to calculate.

15 N-p-tau181, phosphorylated tau181 measured using the Simoa pTau-181 V2.1 Assay kit  
16 (Quanterix); mid-p-tau181, phosphorylated tau181 measured using the originally  
17 developed immunoassay directed to both N- and C-terminally truncated p-tau181  
18 fragments.

19

20 **Figure 5. Comparative analyses of blood biomarkers across the clinical diagnosis**  
21 **groups and between the amyloid PET status.**

22 (A) The data distribution is portrayed using scatter plots, with group differences having  
23 been evaluated through the Kruskal–Wallis test. Statistically significant differences are  
24 denoted as follows:  $p < 0.0001$  (\*\*\*\*),  $p = 0.0004$ , or  $0.0010$  (\*\*\*),  $p = 0.0070$  (\*\*),  
25 and non-significant at  $p < 0.05$  (ns), as determined using Dunn's multiple comparisons.

26 (B) ROC curves were utilized to differentiate AD from other groups determined  
27 according to qualitative findings of amyloid PET. The corresponding AUC values are  
28 listed.

29 CN, cognitively normal; AD, Alzheimer's disease; PSP, progressive supranuclear palsy;  
30 FTL, frontotemporal degeneration; A $\beta$ , amyloid beta; N-p-tau181, phosphorylated  
31 tau181 measured with the Simoa pTau-181 V2.1 Assay kit (Quanterix); mid-p-tau181,  
32 phosphorylated tau181 measured using the originally developed immunoassay directed  
33 to both N- and C-terminally truncated p-tau181 fragments; NfL, neurofilament light  
34 chain; ROC, Receiver Operating Characteristic; AUC, area under the ROC curve.

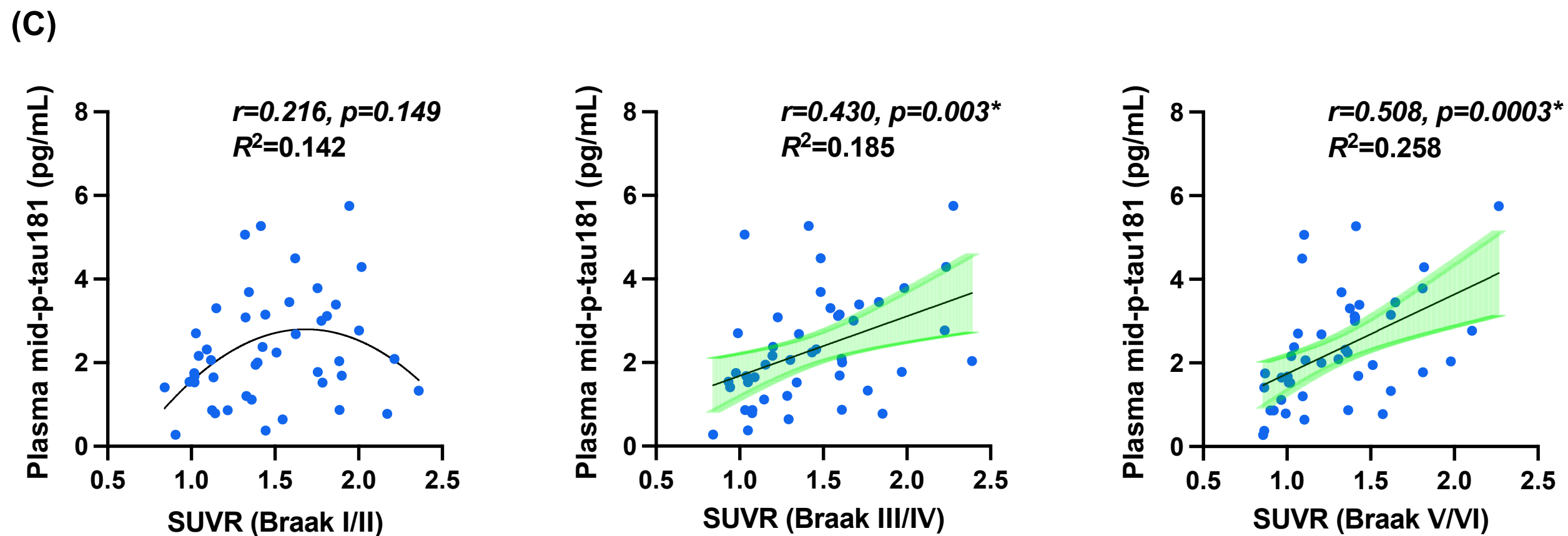
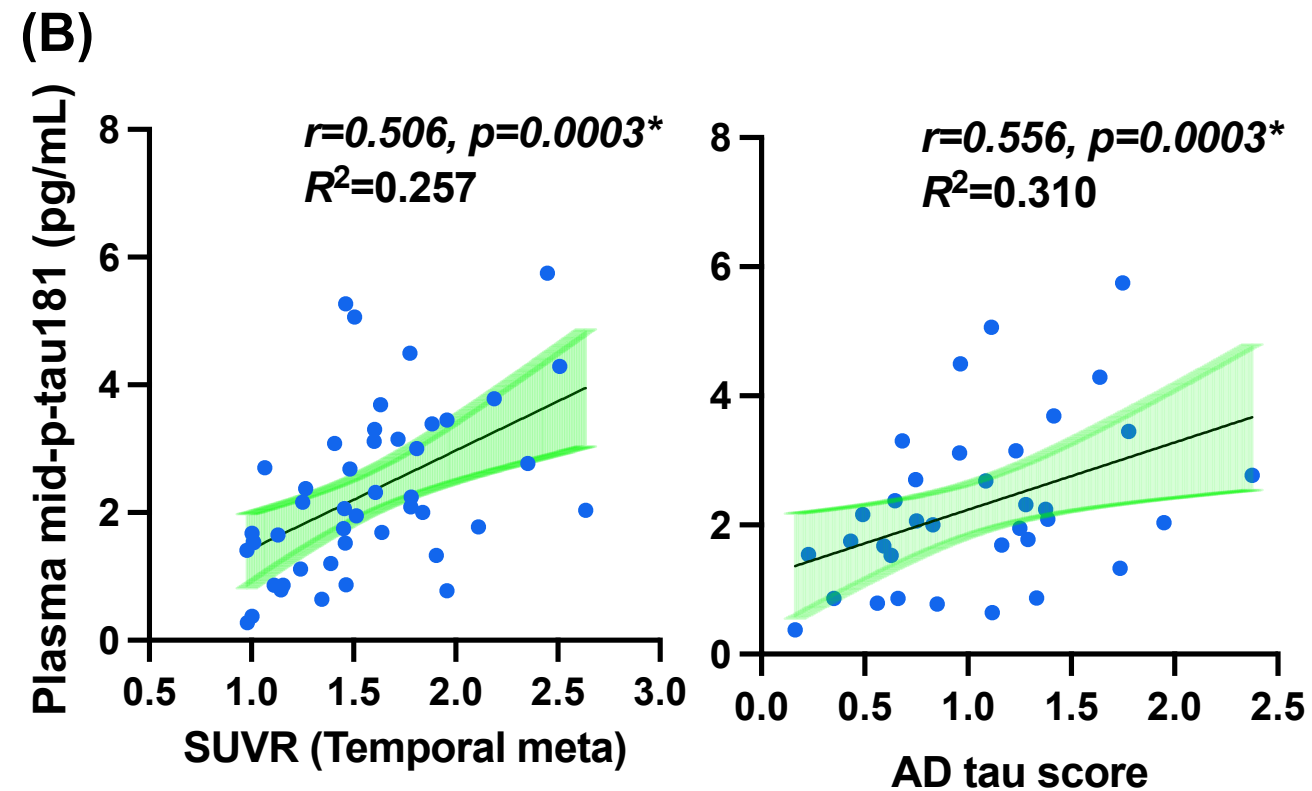
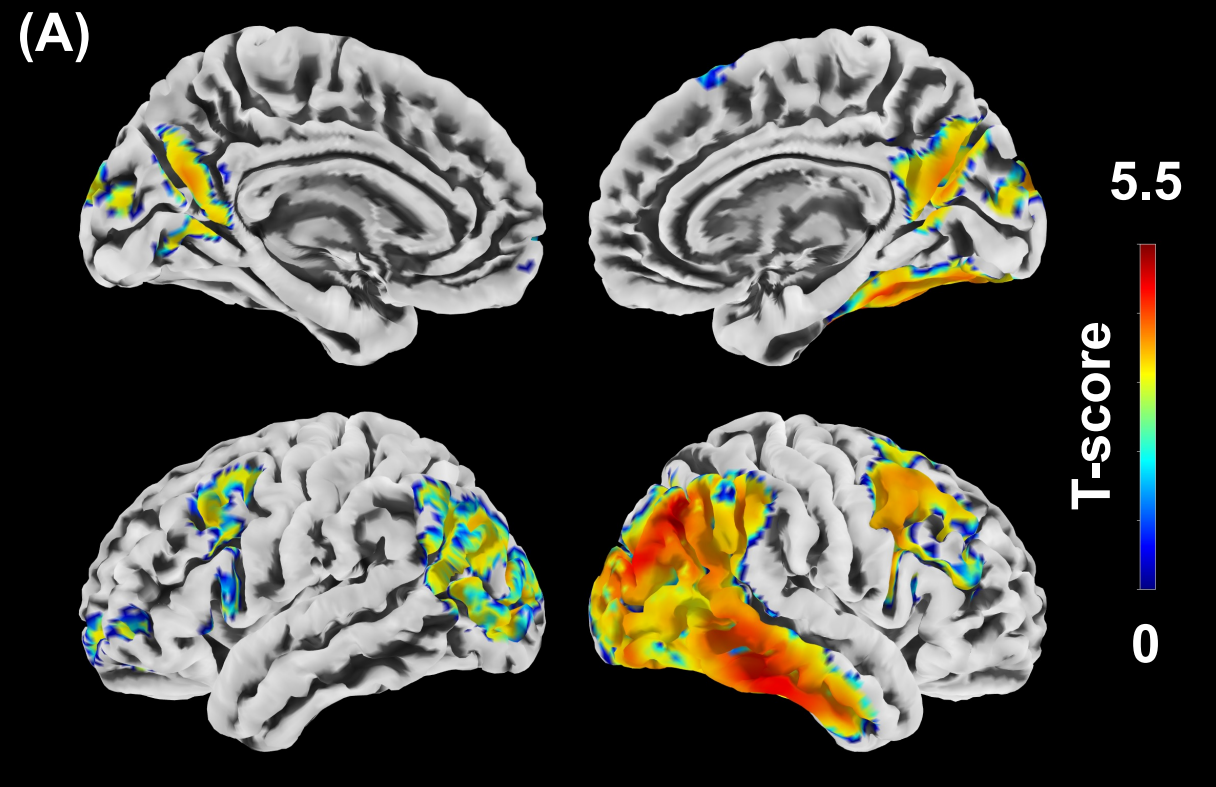
35

1 **Figure 6. Trajectories of the imaging and plasma A/T/N biomarkers along with the**  
2 **decline in the MMSE scores.**

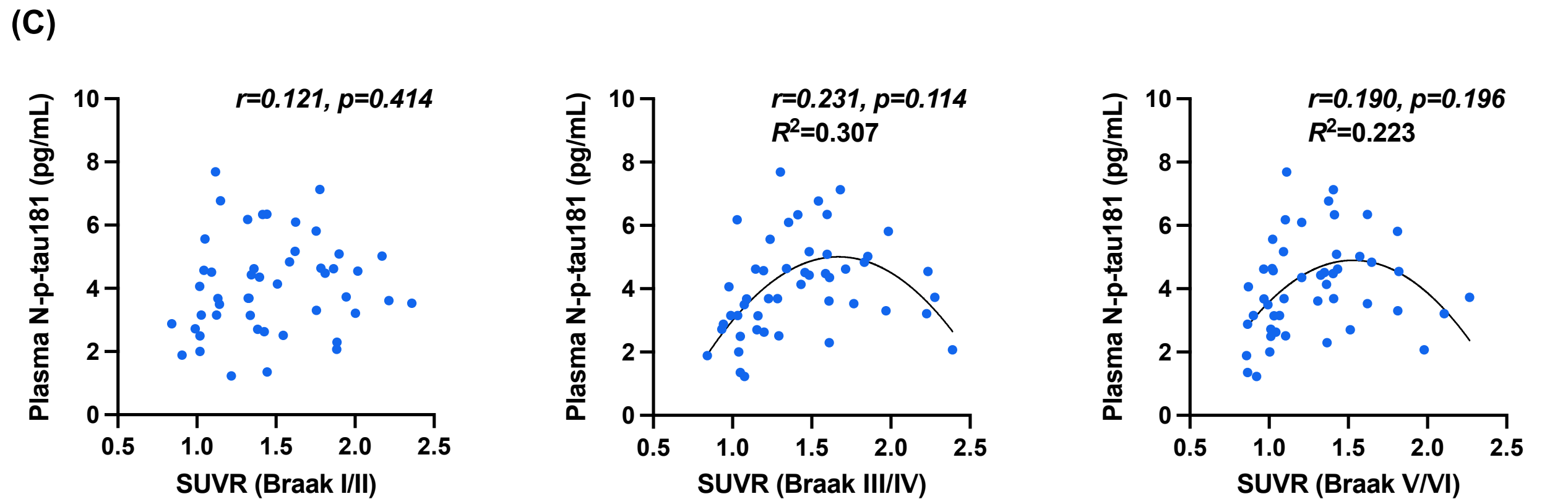
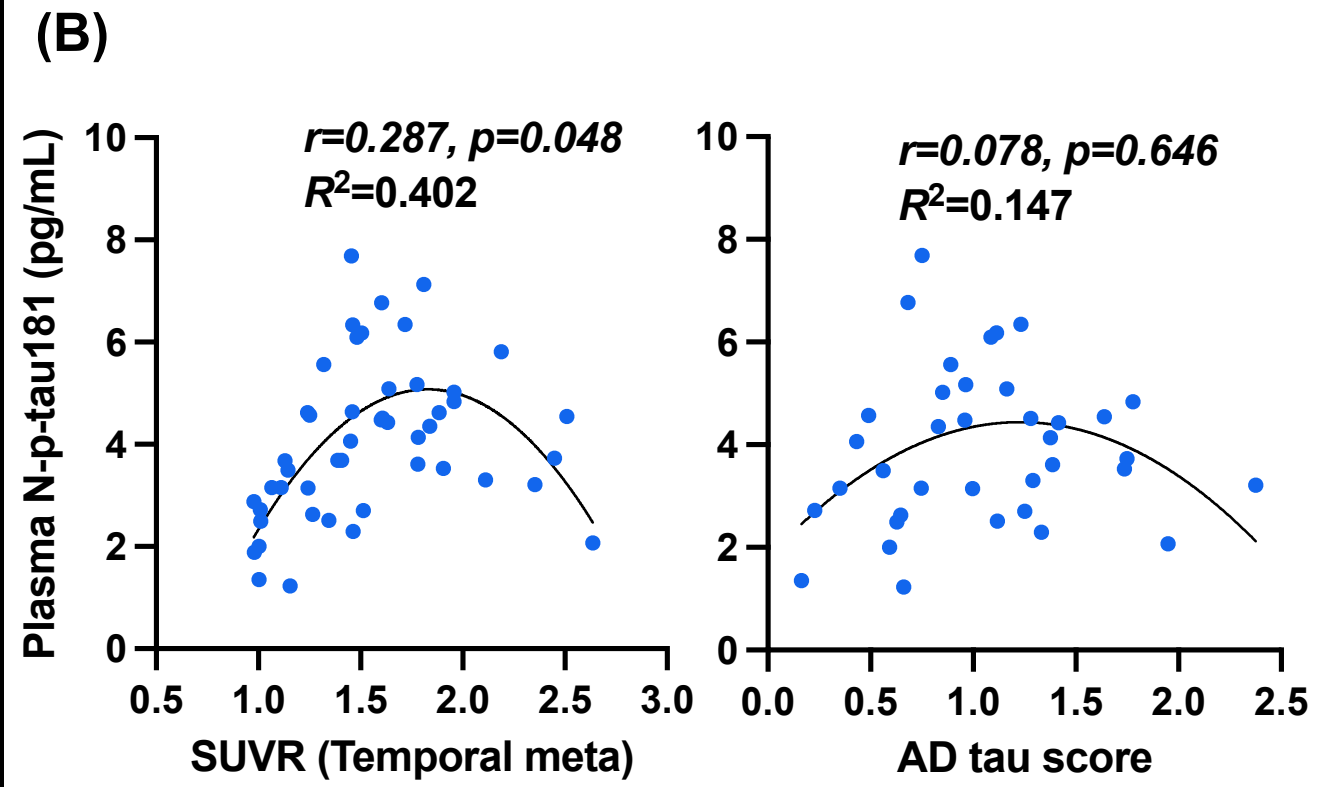
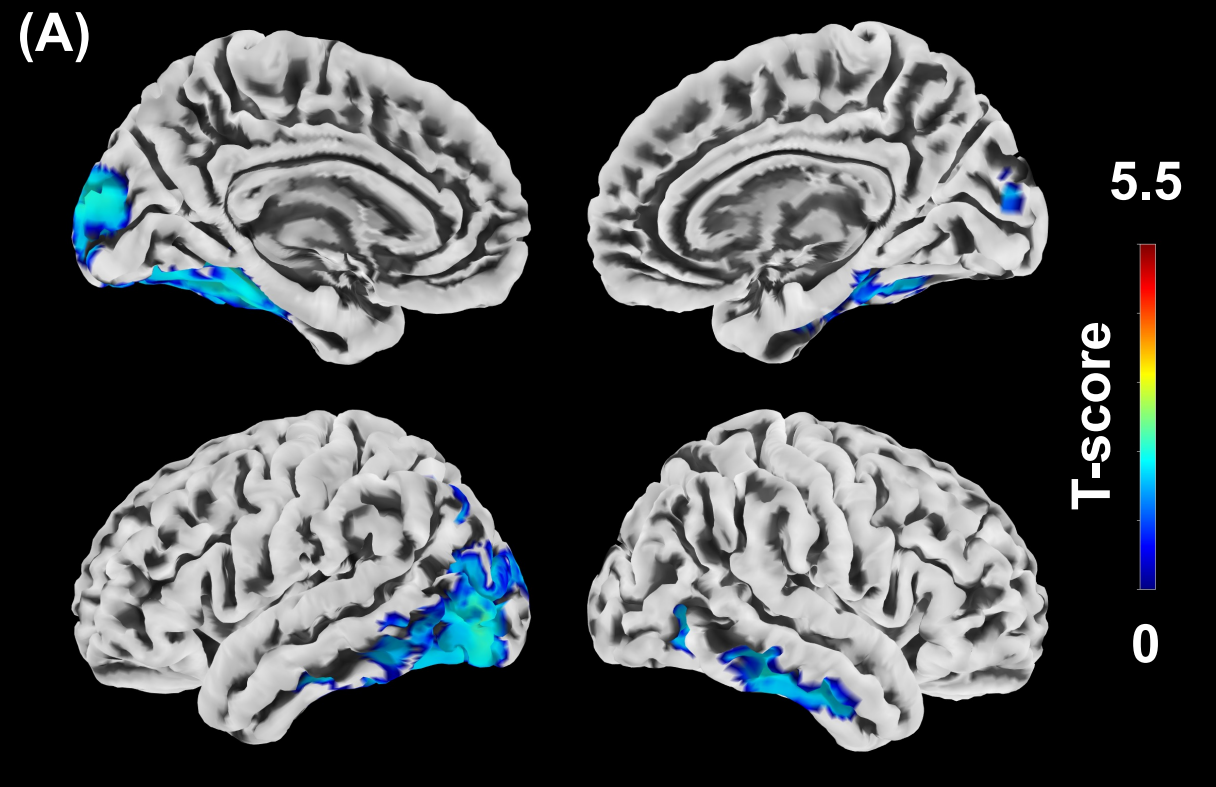
3 Trajectories of the changes in imaging (A) and blood-based (B) A/T/N biomarkers with  
4 the decline in MMSE scores. The relationship between MMSE scores of the CN and AD  
5 continuum subjects and the z-scores of each biomarker is presented as a regression line  
6 that is either straight or sigmoidal, with the best fitting model being selected. The  
7 biomarkers were distinguished using red, green, and blue for both imaging and  
8 blood-based biomarkers, whereas N-p-tau181 was presented separately in purple. The  
9 dotted line indicates z-score = 1.

10

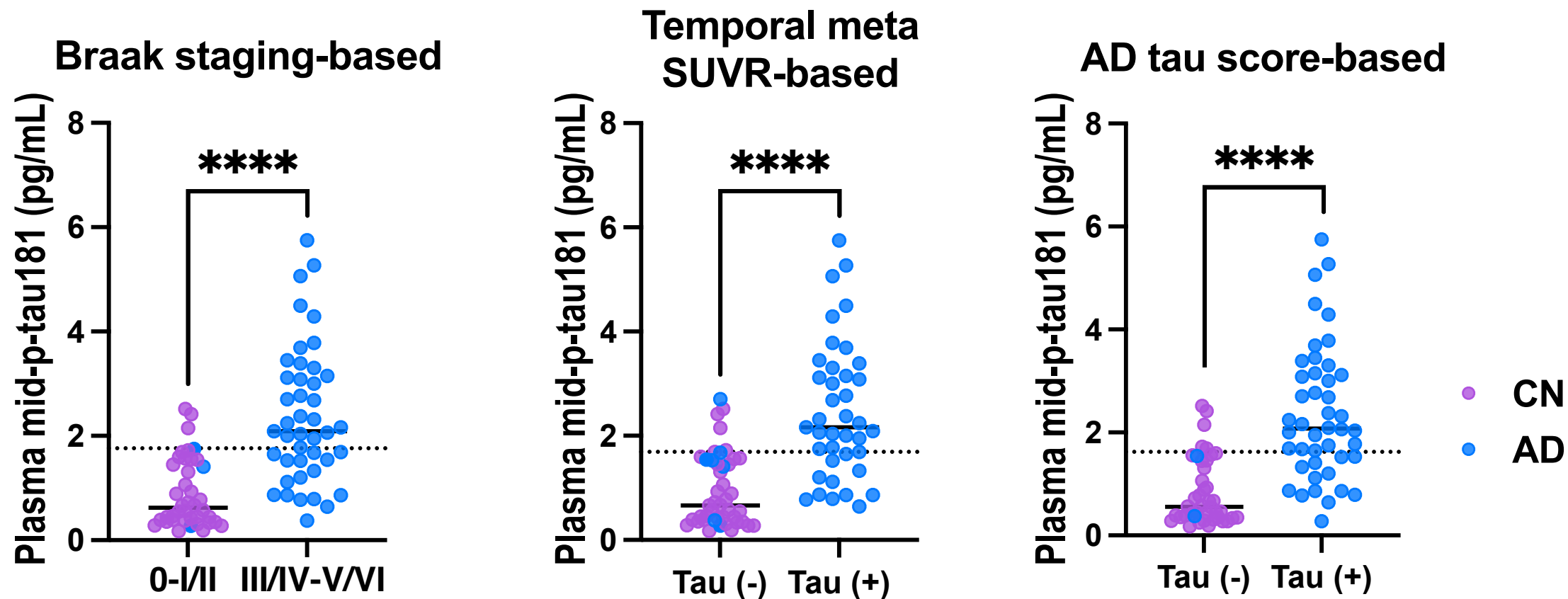
# Tau PET vs Plasma Mid-p-tau181



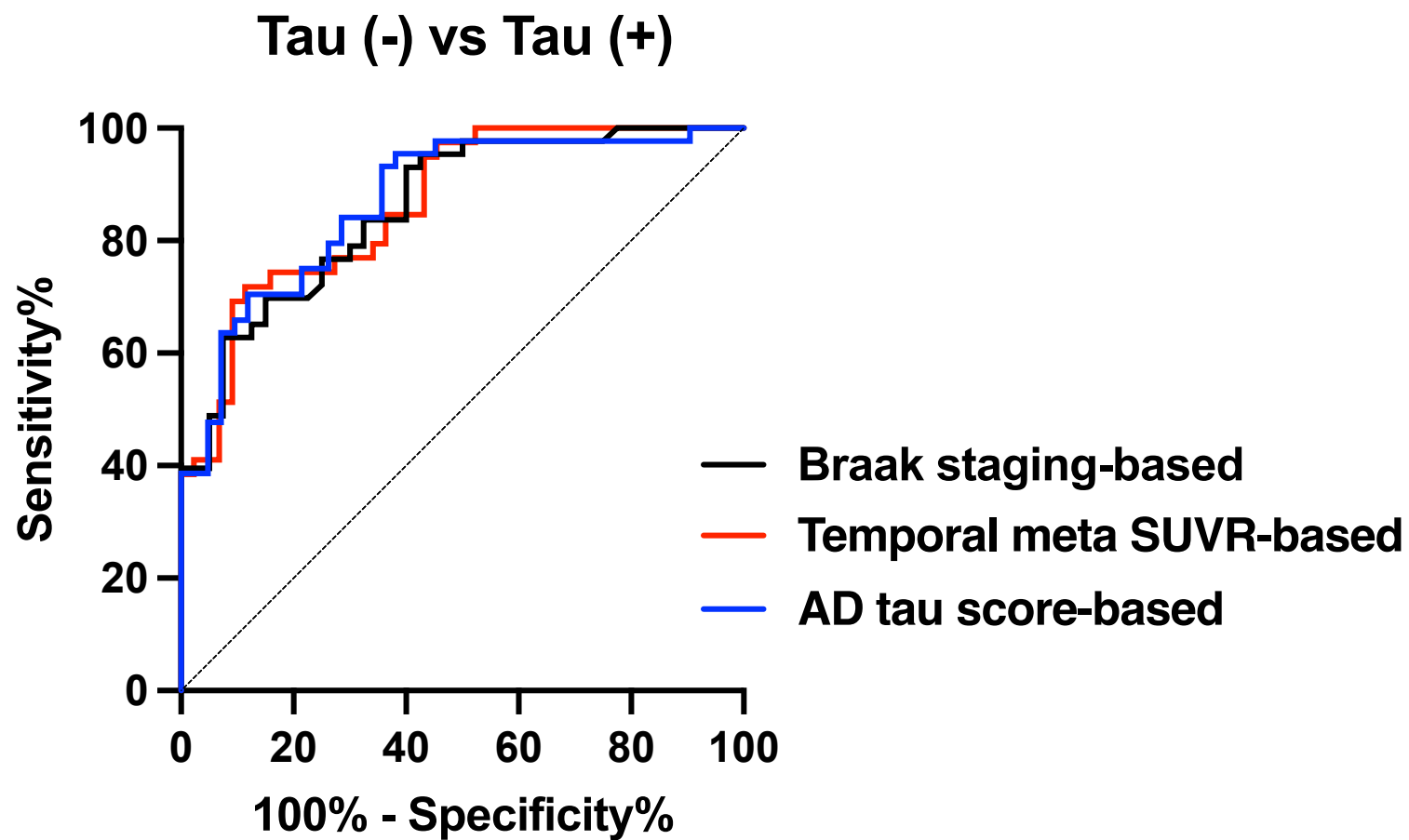
# Tau PET vs Plasma N-p-tau181



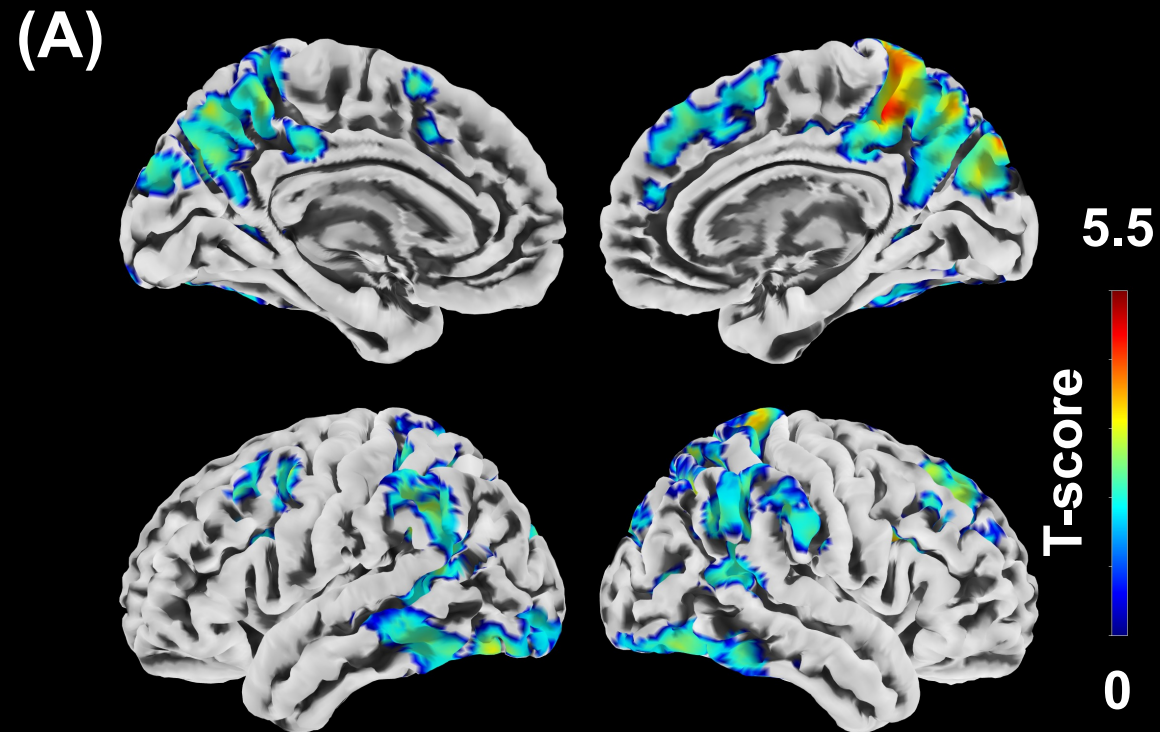
(A)



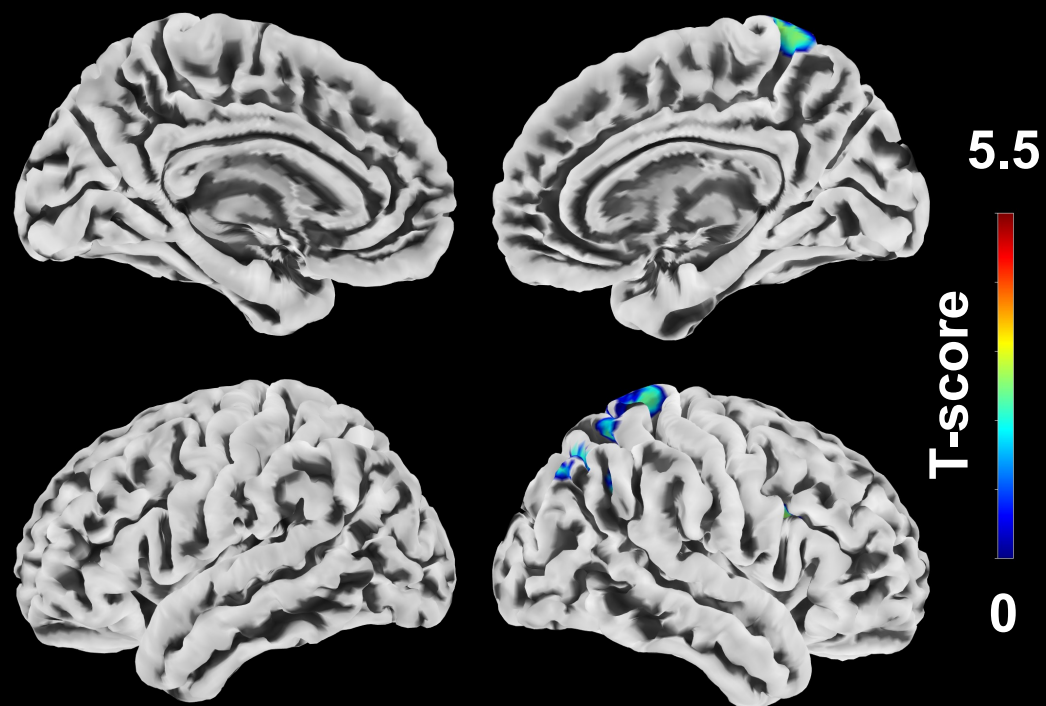
(B)



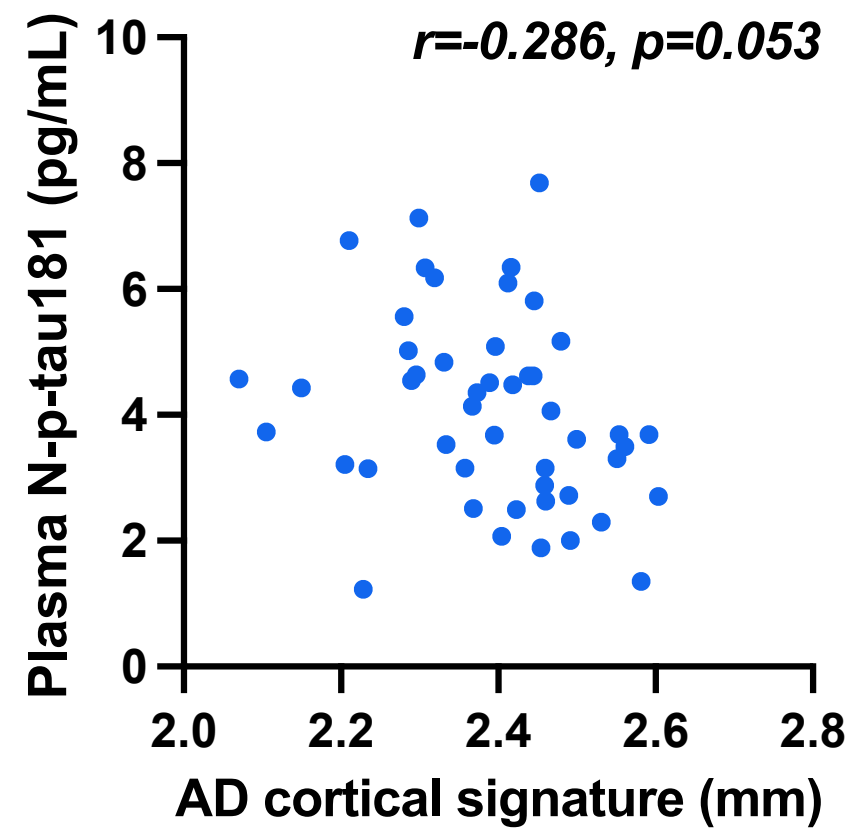
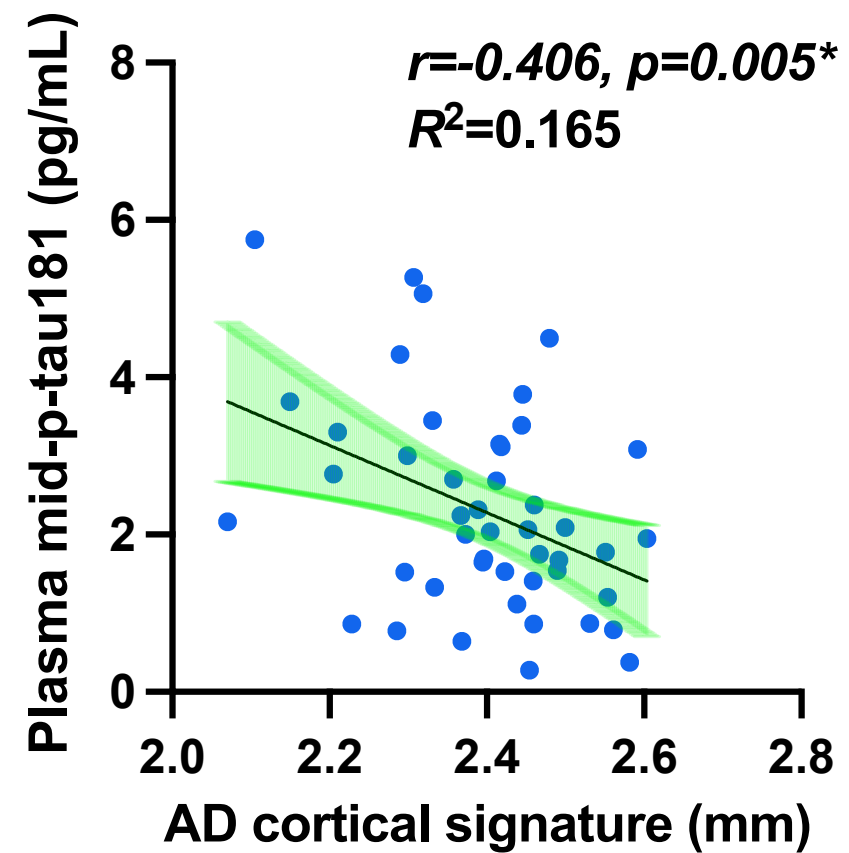
# MRI vs Plasma Mid-p-tau181

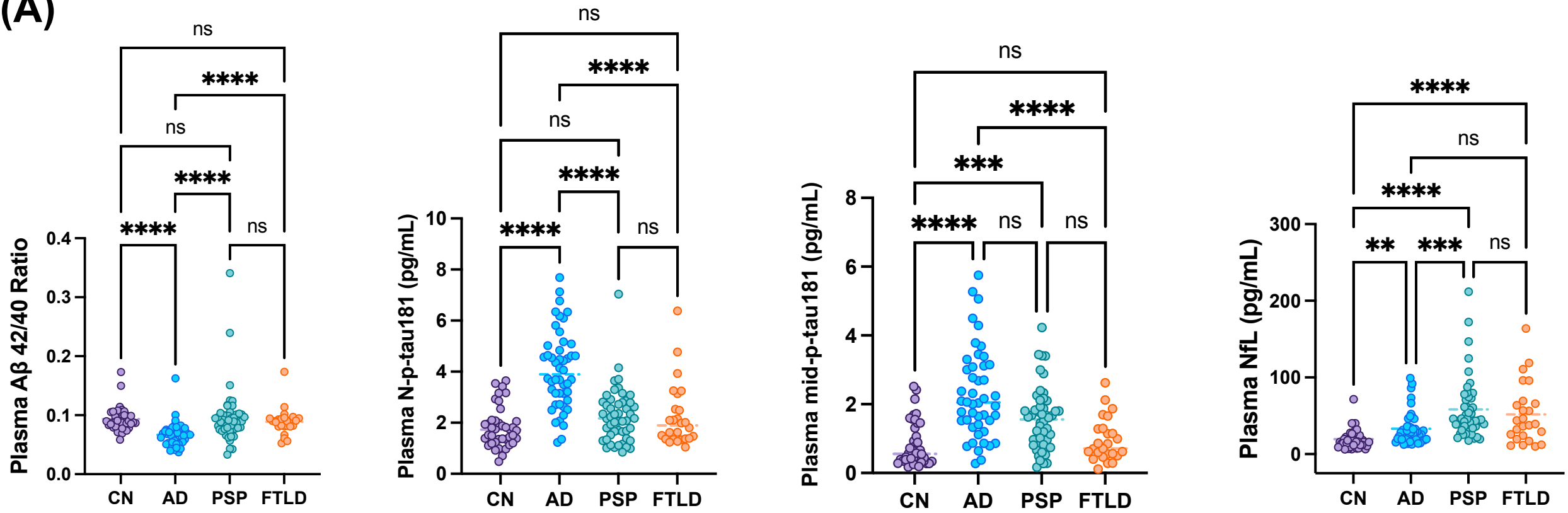
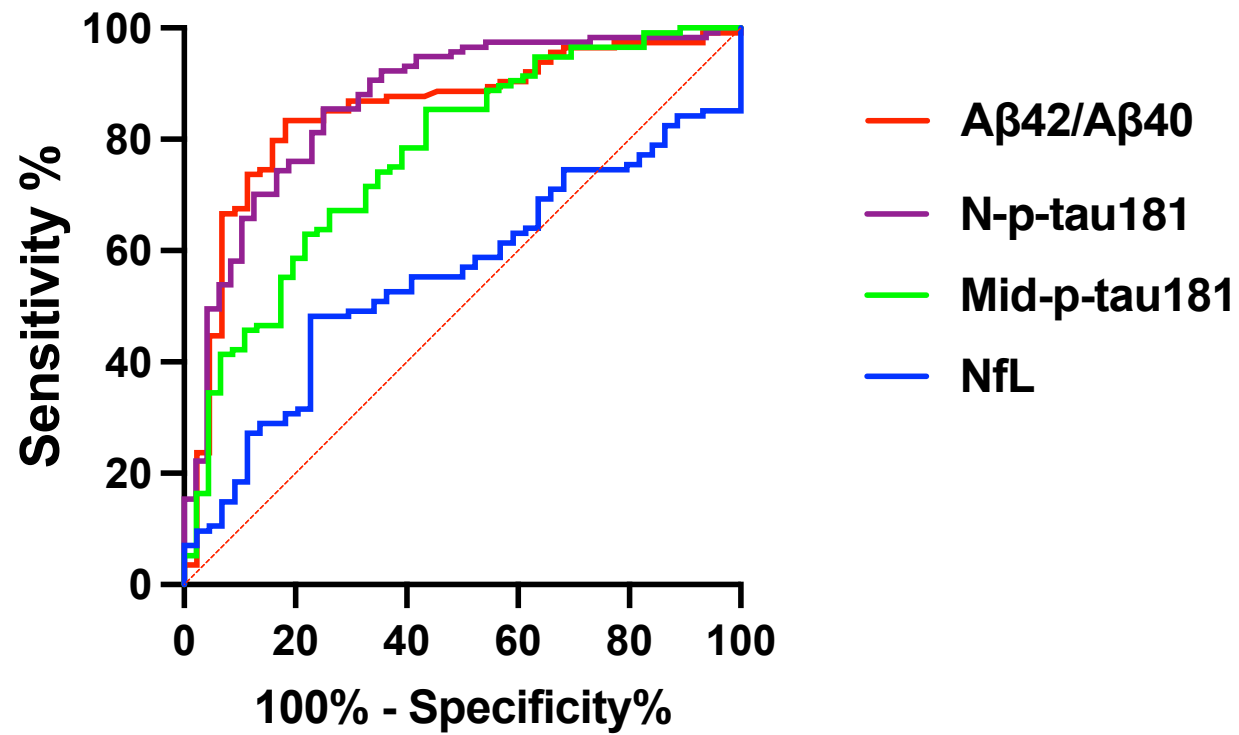


# MRI vs Plasma N-p-tau181



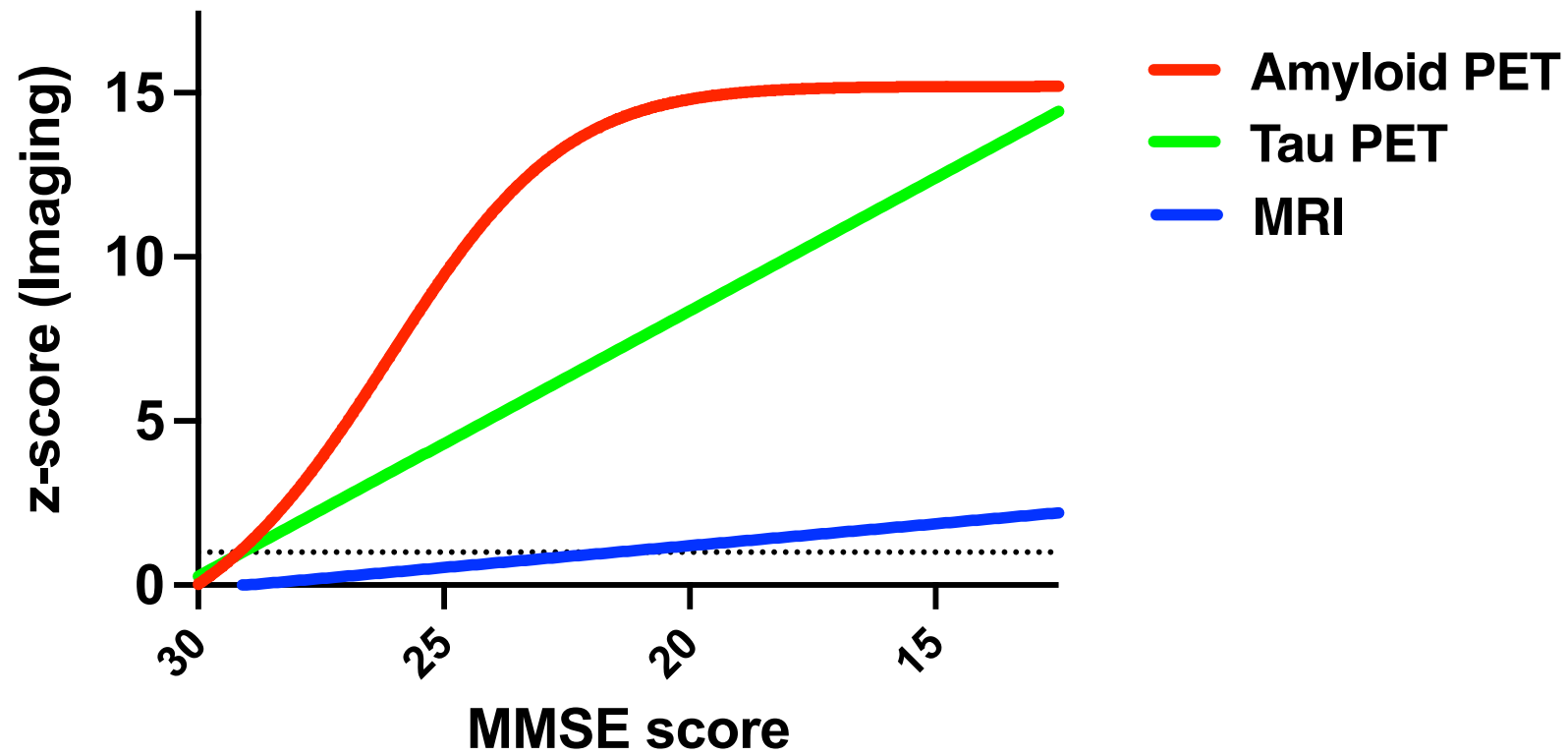
(B)



**(A)****(B)****Amyloid (+) vs Amyloid (-)**

	AUC values
Aβ42/40	0.714
N-p-tau181	0.905
Mid-p-tau181	0.844
NfL	0.641

(A)



(B)

